

# Structural performance of cold-formed high strength steel tubular columns

Han Fang<sup>a</sup>, Tak-Ming Chan<sup>a,\*</sup> and Ben Young<sup>b</sup>

<sup>a</sup>Department of Civil and Environmental Engineering, The Hong Kong Polytechnic University, Hung Hom, Hong Kong, China

<sup>b</sup>Department of Civil Engineering, The University of Hong Kong, Pokfulam Road, Hong Kong, China

\*tak-ming.chan@polyu.edu.hk

## Abstract

This paper presents a numerical investigation into the structural performance of cold-formed high strength steel tubular columns with square, rectangular and circular cross-sections. A finite element model was developed and validated against experimental results on the cold-formed high strength steel tubular columns. Parametric studies using the validated finite element model were carried out to determine the strengths of cold-formed tubular columns with various cross-sectional dimensions, member slenderness values, geometric imperfections and steel grades of S700, S900 and S1100. It was found that increasing the steel grade of the columns led to higher normalised column strengths which were less severely affected by geometric imperfections. The effect of material tensile strength to yield strength ratio on the column strengths was found to be insignificant. Based on the experimental results in literature and the results obtained from parametric studies, the applicability of the design rules in European, Australian and American Standards to cold-formed high strength steel tubular columns was evaluated. The reliability of the design rules was also assessed by performing reliability analysis. The design rules in these standards provide conservative predictions for the strengths of cold-formed high strength steel tubular columns. Recommendations on the column buckling curve selection are discussed. An improved column buckling curve expression considering the increment in normalised column strength with increasing steel grade is also proposed.

**Keywords:** Cold-formed, column strength, design, finite element modelling, high strength steel, tubular columns

## 1. Introduction

High strength steel (HSS) with yield strength (0.2% proof stress) above 460MPa and up to 1100MPa has been produced and increasingly applied to civil structures used as building columns [1] and in bridge structures [2]. HSS structural members demonstrate higher strength-to-weight ratios than the structures formed by conventional-strength steel. Thus, the application of HSS structural members reduces the weight of steel consumption in construction and consequently brings cost and resources savings. Current design codes including European [3-4], American [5] and Australian standards [6-7] allow the design of structures with steel grades up to S700 with nominal 0.2% proof stress of 700MPa, but no specifications for structural members with steel grades higher than S700 are provided in these design codes. Besides, the design rules applied to HSS structures based on European and American standards are the same as those for the structures with steel grades up to S460 and have been developed based on the data for conventional-strength steel members [8-9]. However, the behaviour of HSS members is different from that of conventional strength steel members since the material properties and the ratio of residual stress over yield strength in HSS members are different from those of conventional strength steel members [10-14]. Therefore, applying the same design rules to HSS members with the members made of conventional strength steel may lead to inaccurate structural designs [15-16].

The current study aims to contribute to developing accurate design rules for cold-formed HSS tubular columns with high local buckling resistance, high torsion resistance and ease of fabrication. Research studies have been conducted to investigate the flexural buckling behaviour of cold-formed HSS tubular columns. Somodi and Kövesdi [17] conducted experimental and numerical investigations on the flexural buckling behaviour of cold-formed HSS square tubular columns with steel grades between S420 and S960. The normalised strengths of cold-formed HSS columns were found to be higher than those of the conventional-strength steel columns since the ratios of the average residual stress over yield strength in HSS members are lower [10]. It has also been found that the design specification in European standard [3] provides conservative strength predictions for the cold-formed HSS square tubular columns. Dundu and Chabalala [18] investigated the strength of cold-formed circular tubular columns made of steel with 0.2% proof stress ranging from 484.7 to 503.7MPa. The column strengths were found to be higher than the strengths estimated based on the design specification in European code. Ma [19] experimentally investigated the structural behaviour of four cold-formed HSS tubular columns with square, rectangular and circular cross-sections made of S700 or S900 steel while Javidan et al. [20] tested two cold-formed S700 and S1100 steel columns with circular cross-section. Each of these studies focused on an individual cross-section shape or limited steel grades. The results in these studies also reveal that quite limited data were obtained for the cold-formed tubular columns with the steel grade of S1100. For each cross-section shape, no systematic

studies have been carried out to investigate the behaviour of the columns with various steel grades up to S1100. The experimental and numerical data in these studies are insufficient for developing accurate design rules for the cold-formed HSS columns with various cross-section shapes and with steel grades up to S1100.

Therefore, in the current study, a numerical investigation into the structural performance of cold-formed S700, S900 and S1100 tubular columns with square hollow sections (SHS), rectangular hollow sections (RHS) and circular hollow sections (CHS) was conducted. A finite element (FE) model was developed and validated against test results. Subsequent parametric studies on the cold-formed HSS tubular columns with various cross-sectional dimensions and member slenderness values were conducted using the validated FE model. Based on the experimental results in literature and the parametric studies results, the applicability and reliability of the design rules in European, Australian and American standards, on the cold-formed HSS tubular columns was evaluated. Recommendations on column buckling curve selection for design rules in standards and a new column buckling curve expression were proposed.

## 2. Finite element modelling and validation

Finite element (FE) modelling using the software package ABAQUS 6.12 [21] was carried out to investigate the structural performance of cold-formed HSS columns with square, rectangular and circular hollow sections, and to obtain column strength data for the development of accurate design rules. A finite element model was first developed and validated using the test results of cold-formed HSS tubular columns [17-20]. The labels and dimensions of the columns investigated in these studies are presented in Table 1 for SHS and RHS columns and in Table 2 for CHS columns using the nomenclature defined in Fig. 1. The yield strength ( $f_y$ ) and ultimate strength ( $f_u$ ) of the column materials and the test results of ultimate loads ( $N_{u, test}$ ) of the columns are also provided in the tables. In the following Sections 2.1 and 2.2, the FE model and its validation are presented.

### 2.1 Description of the FE model

The cold-formed HSS tubular columns were modelled using the four-noded S4R shell element with reduced integration. This type of element has been successfully used in the accurate FE modelling of steel tubular columns [22-24]. The mesh size of  $(B+H)/30$  was adopted for the SHS and RHS columns while the mesh size for CHS columns was  $D/15$ . Measured material stress-strain curves for the columns were reported in the experimental studies [17, 19-20]. For the CHS columns investigated by Dundu and Chabalala [18], material properties were presented while no measured stress-strain curves were provided. Thus, the stress-strain model proposed by Ma et al. [25] for cold-formed high strength steel CHS members was adopted and stress-strain curves were subsequently obtained by substituting

the material properties measured by Dundu and Chabalala [18] in the model. These measured and calculated stress-strain curves were converted into the true stress-log plastic strain curves using Eqs. (1) and (2). The obtained true stress-log plastic strain curves were subsequently incorporated into the FE model.

$$\sigma_{true} = \sigma(1 + \varepsilon) \quad (1)$$

$$\varepsilon_{ln}^{pl} = \ln(1 + \varepsilon) - \frac{\sigma}{E} \quad (2)$$

In Eqs. (1) and (2),  $\varepsilon_{ln}^{pl}$  is the logarithmic plastic strain,  $\varepsilon$  is the engineering strain,  $E$  is the Young's modulus, and  $\sigma_{true}$  and  $\sigma$  are the true stress and engineering stress respectively. For cold-formed SHS and RHS columns, material strength enhancements at the corner regions were obtained due to the cold-working effect caused by the cold-forming fabrication process, as shown in Table 1. It has also been found that the strength enhancements also occur at the flat portions adjacent to the corners [26-29]. Extending the corner material properties to the flat portions adjacent to corners with the width of two times the cross-section thickness on each side of a corner region can be applied to account for the strength enhancements at these locations [26-29]. This finding was adopted in this study for modelling cold-formed SHS and RHS columns.

Initial local and global geometric imperfections exist in the column structures and can affect the buckling behaviour and strengths of the columns. Thus, both local and global geometric imperfections were included in the FE model. The lowest local and global eigenmode shapes obtained by conducting separate linear eigenvalue buckling analysis were used as the local and global geometric imperfection patterns respectively. The scaled local and global eigenmode shapes with the magnitudes of the local and global imperfections respectively were assigned to the column FE model. For the SHS columns from the study of Somodi and Kövesdi [17], local and global geometric imperfection magnitudes of  $0.7*B/1000$  and  $1/1000$  of column length respectively were provided in the study and adopted for the modelling. For the H 80\*80\*4-LBC, H 50\*100\*4-LBC and H 100\*50\*4-LBC columns in Table 1, the local geometric imperfection magnitudes provided as  $0.0119*(B-2R)*t$  [19] were used while the measured global geometric imperfection magnitudes of  $1/3885$ ,  $1/58268$  and  $1/6474$  of column length were adopted [19]. For the V89\*3-LBC CHS column, local and global geometric imperfection magnitudes of  $0.0058D/t$  and  $1/9711$  of column length respectively [19] were used for the FE modelling. However, Dundu and Chabalala [18] only reported the geometric imperfection measured at mid-height of the columns while Javidan et al. [20] only reported the global geometric imperfection magnitudes of about  $1/1000$  column length for S-HST2 and S-UHST2. For the 165.1\*3.0L1500, 165.1\*3.0L2000, 220.0\*3.5L2000 and 220.0\*3.5L2500 columns without determining the global imperfection magnitude due to the maximum initial out-of-straightness along each column length and loading eccentricity, the global imperfection magnitudes of  $1/2500$ ,  $1/2000$ ,

1/1500 and 1/1000 of column length were used in the analysis. The behaviour of the columns estimated using these global imperfection magnitudes was compared with that obtained from experiments in order to obtain the global imperfection magnitudes for the columns. The local imperfection effect was also taken into account in the FE models for CHS columns tested in experiments [18, 20], and the local imperfection values suggested by Ma et al. [29] based on the measurements of local geometric imperfections for cold-formed CHS columns made of high strength steel were adopted and equal to  $0.0058D/t$ .

Longitudinal residual stresses also exist in the cold-formed tubular columns due to cold-forming and welding and have the most influence on the structural behaviour. The longitudinal residual stresses composed of bending and membrane residual stresses and have been measured for cold-formed HSS tubular columns [10, 25]. It has been found that the bending residual stresses are much larger than the membrane residual stresses. The effect of bending residual stresses was inherently included in the measured material properties since the specimens extracted from the cold-formed tubular structures for material properties measurements were initially curved due to the release of bending residual stresses and subsequently straightened during the tensile testing [19, 26, 30-31]. The membrane residual stresses were found to be below 20% of the 0.2% proof stress [10, 25]. Owing to the low magnitudes of the membrane residual stresses, their effect on the strength of cold-formed HSS columns was quite limited [10, 25]. Thus, the inclusion of membrane residual stresses in the FE model for column structures was unnecessary.

Boundary conditions employed in the tests for the columns were also replicated in the FE model. The nodes of each end surface of any column were coupled with a reference point. For the reference point on the unloaded side, all degrees of freedoms were restrained, except for the rotation about the buckling axis. The boundary conditions applied to the reference point on the loaded side was the same as those for the reference point on unloaded side, except that the longitudinal displacement was allowed. Typical boundary conditions defined for the CF7-R150\*8\_1B column are presented in Fig. 2. For S-HST2 and S-UHST2 columns, the rotations at the reference points were also restrained to simulate the fixed-end conditions applied in the tests [20]. Loading was applied by specifying the rate of longitudinal displacement at the reference point on the loaded side. The above described FE model for any column was solved using the modified Riks method to obtain the load-displacement behaviour of the structure including the post-ultimate behaviour.

## 2.2 Validation

The FE model introduced in Section 2.1 was validated against the experimental results of columns listed in Tables 1 and 2. The FE modelling results of the column strengths ( $N_{u,FE}$ ) were firstly compared with the experimental results ( $N_{u,test}$ ), as shown in Fig. 3 for SHS, RHS and CHS columns.

As can be seen in the figure, the column strengths estimated by FE modelling are in excellent agreement with those from experimental investigations. For SHS and RHS columns, the mean value of the  $N_{u,FE}/N_{u,test}$  ratio was estimated to be 1.00, with the coefficient of variation (COV) of 0.03. As for the CHS columns, the mean value of  $N_{u,FE}/N_{u,test}$  ratio was also estimated to be 1.00, with the COV of 0.016. For the 165.1\*3.0L1500 and 165.1\*3.0L2000 columns, it was found that the  $N_{u,FE}$  estimated using the global imperfection of 1/1500 of column length compared well with the corresponding  $N_{u,test}$ . As for the 220.0\*3.5L2000 and 220.0\*3.5L2500 columns,  $N_{u,FE}$  estimated using the global imperfection of 1/1000 of column length compared well with the corresponding  $N_{u,test}$ .

The load-displacement behaviour estimated in FE modelling for the columns were also compared with the experimental results. Typical load-mid deflection curves obtained from FE modelling for the RHS columns are presented in Fig. 4 in comparison with the curves from experiments. Typical load-axial displacement curves obtained from FE modelling for the CHS columns are presented in Fig. 5 together with the curves obtained from experiments. The global buckling failure mode obtained for the H 50\*100\*4-LBC and S-HST2 columns from FE modelling was compared with that observed in experiments, as shown in Figs. 6 and 7 respectively. As can be observed in Figs. 4-7, the FE modelling results of load-displacement behaviour and failure modes of the columns compared well with those experimental results.

### 3. FE Parametric studies

#### 3.1 General

A series of parametric studies were carried out using the validated FE model to investigate the performance of pin-ended cold-formed S700, S900 and S1100 tubular columns and to generate further data of the column strengths for developing accurate design approaches. Effects of geometric imperfection, steel grade and ratio of material tensile strength over yield strength ( $f_u/f_y$  ratio) on the strengths of cold-formed SHS, RHS and CHS columns were examined. A variety of parameters relating to the cross-sectional dimension, member slenderness and buckling direction were considered in the parametric studies. The values for these parameters are provided in Table 3. As can be seen in the table, varying plate thicknesses were selected for the columns in order to obtain the class 1-3 cross-sections according to the cross-sectional classification specifications in European standard [3]. The member slenderness values between 0.45 and 2.6 were calculated according to the specification provided in the European standard [3]. Besides, buckling about both major and minor axes was considered for the RHS columns.

Initial geometric imperfections were applied to columns in the FE modelling. The average global geometric imperfection measured for the SHS and RHS columns in Table 1 equal to 1/1580 of the

column length while the average magnitude of global geometric imperfection for the CHS columns in Table 2 is  $1/1280$  of the column length. These average magnitudes of the global geometric imperfection for the SHS, RHS and CHS column members were adopted in the parametric studies to investigate the strengths of columns with varying steel grades and  $f_u/f_y$  ratios, and to generate data of column strengths for evaluating the suitability of existing design rules for the columns, as shown in Table 3. Different global geometric imperfection magnitudes of  $1/1000$  and  $1/2000$  of column length were also used in order to quantify the effect of global geometric imperfection, as presented in Table 3. The strengths of columns estimated using varying global geometric imperfections were compared, as presented in Section 3.2. Since the cross-sections selected for parametric studies are relatively stocky, no incorporation of local geometric imperfections was made.

The material properties measured by Ma et al. [25] for cold-formed HSS tubular members made of S700, S900 and S1100 were used for the parametric studies. The stress-strain curves for the FE parametric studies were obtained using the stress-strain curve model proposed in the study of Ma et al. [25], with the substitution of material parameters given in their study. The material parameters taken as the average values from material properties measurements are presented in Table 4. Typical stress-strain curves for both flat and corner materials are shown in Fig. 8. As can be seen in the figure, strength enhancements were obtained for corner materials and subsequently taken into account for the SHS and RHS columns according to the arrangement introduced in Section 2.1. Since the material properties and stress-strain curves were obtained based on testing the materials extracted from cold-formed tubular members [25], the effect of bending residual stresses has been inherently accounted in these properties, as discussed in Section 2.1. The material properties results obtained in the study of Ma et al. [25] also show that the  $f_u/f_y$  ratio actually varies for tubular columns in each steel grade. Therefore, effect of  $f_u/f_y$  ratio on the column strengths was also examined, as illustrated in Section 3.4. The upper and lower limits for the  $f_u/f_y$  ratio based on material properties measurements [25] are also given in Table 4.

### 3.2 Effect of global geometric imperfection

The effect of global geometric imperfection on the strengths of cold-formed HSS tubular columns was investigated in this section. For this investigation, the parameters for the SHS, RHS and CHS columns relating to their steel grade, dimensions, member slenderness and buckling direction are given in Table 3. The columns with different global geometric imperfection magnitudes shown in Table 3 were modelled. The obtained column strengths normalised by the cross-sectional capacity ( $\chi_{FE}$ ) are presented in Figs. 9-11 for S700, S900 and S1100 columns respectively. As can be seen in the figures, the normalised column strengths are affected by the magnitudes of global geometric imperfection and decrease with increasing global geometric imperfection magnitude. The effect of global geometric

imperfection was also found to be related to the column slenderness and is the largest with the column slenderness value of about 1.3, 1.2, 1.2 and 1.2 for SHS columns, RHS columns buckling about major and minor axes and CHS columns respectively. The maximum reduction of normalised column strength with increasing global geometric imperfection from 1/2000 to 1/1000 of column length is lower for the columns with a higher steel grade. For all columns with SHS, RHS and CHS, the average reduction of column strength due to increasing global geometric imperfection from 1/2000 to 1/1000 of column length is 4.0, 3.2 and 2.8% for S700, S900 and S1100 columns respectively.

### 3.3 Effect of steel grade

The effect of steel grade on the strengths of the cold-formed HSS tubular columns was investigated. For each cross-section shape and steel grade, columns with ten member slenderness values between 0.45 and 2.6 were selected for the investigation. The average global geometric imperfection magnitudes of 1/1580 of the column length for SHS and RHS columns and 1/1280 of the column length for CHS columns were used. The FE results of normalised column strengths are plotted against member slenderness values, as shown in Fig. 12. In the figures, it can be observed that the normalised column strengths increase with the increasing steel grade. Comparing with the S700 columns, the normalised column strengths increased by 0.5-4.2% and 1.0-7.4% for S900 and S1100 columns respectively. It is also revealed in the figures that the increment of normalised column strengths with increasing steel grade is related to the member slenderness. The strength increment is higher for the columns with member slenderness between 0.7 and 1.2. The higher normalised strengths for columns with a higher steel grade can be due to the relatively lower bending residual stresses on average, comparing with the yield strength of the material in the columns [10]. In addition, the increment of normalised column strengths with increasing steel grade from S700 to S1100 is also caused by the less severe effect of global geometric imperfection on the column strengths, as illustrated in Section 3.2.

### 3.4 Effect of $f_u/f_y$ ratio

The effect of  $f_u/f_y$  ratio on the strengths of the cold-formed HSS tubular columns was also investigated. Strengths of SHS, RHS and CHS columns were estimated with varying ultimate tensile stress of the material to obtain the lower and upper limits of  $f_u/f_y$  ratio in Table 4 and using the average global geometric imperfection magnitudes for the columns. The comparison of the normalised column strengths estimated based on the lower and upper  $f_u/f_y$  ratio limits ( $\chi_{low}$  and  $\chi_{upp}$  respectively) is presented in Fig. 13. The effect of  $f_u/f_y$  ratio is mainly observed for columns with low slenderness between 0.45 and 1.1 since the maximum strains in these columns are larger than the material yield strains. Thus, plastic regions exist in the columns and column strengths are dependent on the strain hardening effect of the material. The maximum difference of normalised column strengths due to the



effect of  $f_u/f_y$  ratio is about 2.2, 2.0, 1.9 and 2.9% for SHS columns, RHS columns buckling about major and minor axes and CHS columns respectively when the member slenderness is about 0.46. The effect of  $f_u/f_y$  ratio reduces with increasing member slenderness, as shown in Fig. 13. For columns with relatively high member slenderness, no effect of  $f_u/f_y$  ratio on the column strengths is observed since elastic buckling occurs and the strains in the columns are below the material yield strain.

## 4. Design approaches

The applicability of the design rules in European, Australian and American standards to cold-formed tubular columns with steel grades from S700 to S1100 was assessed in this section. The column strengths predicted based on the specifications in standards were compared with the column strengths from both experimental investigations conducted by researchers [17, 19-20] and FE parametric studies presented in Section 3. The accuracy and reliability of existing design rules for predicting the strengths of the columns and the selection of column buckling curves were discussed. A new column buckling curve considering the dependency of column strengths on the steel grade was also proposed.

### 4.1 Current design rules

The estimation of the strength of a column under axial compression according to existing design rules is typically conducted by multiplying the strength of the column cross-section,  $A \cdot f_y$ , with a reduction factor  $\chi$  for the buckling of the column. Variations of the reduction factor with the column member slenderness are provided as column buckling curves in different standards.

In the European Standard EC3 [3-4], five buckling curves describing the relationships between the buckling reduction factor ( $\chi_{EC}$ ) and member slenderness are given. Each buckling curve is related to a specific value of imperfection factor  $\alpha$  and is presented in the form given as Eqs. (3)-(5)

$$\chi_{EC} = \frac{1}{\Phi + \sqrt{\Phi^2 - \bar{\lambda}_{EC}^2}} \quad (3)$$

$$\Phi = 0.5 \times [1 + \alpha(\bar{\lambda}_{EC} - 0.2) + \bar{\lambda}_{EC}^2] \quad (4)$$

$$\bar{\lambda}_{EC} = (A \times f_y / N_{cr})^{0.5} \quad (5)$$

where  $\bar{\lambda}_{EC}$  is the member slenderness and  $N_{cr}$  is the elastic critical force for the relevant buckling mode of the member. For cold-formed SHS, RHS and CHS columns, buckling curve c with the imperfection factor  $\alpha$  of 0.49 is recommended for columns with any steel grade up to S700.

Australian Standard AS4100 [6] also employs the multiple column curve concept and provides five buckling curves which are expressed through Eqs. (6)-(9)

$$\chi_{AS} = \xi \left[ 1 - \sqrt{1 - \left( \frac{90}{\xi(\lambda_n + \alpha_a \times \alpha_b)} \right)^2} \right] \quad (6)$$

$$\xi = \frac{\left( \frac{\lambda}{90} \right)^2 + 1 + 0.00326 \times (\lambda_n + \alpha_a \times \alpha_b - 13.5)}{2 \times \left( \frac{\lambda}{90} \right)^2} \quad (7)$$

$$\alpha_a = \frac{2100 \times (\lambda_n - 13.5)}{\lambda_n^2 - 15.3 \times \lambda_n + 2050} \quad (8)$$

$$\lambda_n = \left( \frac{l_e}{r} \right) \sqrt{k_f} \sqrt{\frac{f_y}{250}} \quad (9)$$

where  $\alpha_a$  is the slenderness modifier,  $\lambda_n$  is the modified member slenderness,  $\xi$  is the compression member factor defined in Clause 6.3.3 AS4100,  $l_e$  is the column effective length,  $r$  is the radius of gyration and  $k_f$  is the form factor. The choice of buckling curve is related to the member section constant  $\alpha_b$  and depends on the fabrication route and cross-sectional shape of the tubular columns. For the cold-formed and non-stress relieved tubular columns, the buckling curve for the  $\alpha_b$  value of -0.5 should be used for predicting the column strengths [6].

American standard AISC 360 [5] provides a single column curve. The buckling reduction factor ( $\chi_{AISC}$ ) can be estimated using Eqs. (10) and (11) based on the non-dimensional column slenderness  $\bar{\lambda}_{AISC}$  expressed as Eq. (12). In Eqs. (10) and (11), the two constant terms were obtained for the column design based on experimental data [32-34]. The same equations are also provided in AISI S100 [35] and AS4600 [36] standards for members which are subject to compression. The resistance factor ( $\phi$ ) for AISC 360 standard is 0.9 which is larger than the value of 0.85 provided in AISI S100 and AS4600. Thus, the accuracy and reliability of AISC 360 standard was evaluated and referred to in the following sections.

$$\chi_{AISC} = 0.658^{\bar{\lambda}_{AISC}^2} \quad \text{for } \bar{\lambda}_{AISC} \leq 1.5 \quad (10)$$

$$\chi_{AISC} = \frac{0.877}{\bar{\lambda}_{AISC}^2} \quad \text{for } \bar{\lambda}_{AISC} > 1.5 \quad (11)$$

$$\bar{\lambda}_{AISC} = \frac{l_e}{\pi r} \sqrt{\frac{f_y}{E}} \quad (12)$$

The column buckling curves from EC3, AS4100 and AISC 360 are plotted in comparisons with the column strength data from experiments and FE parametric studies, as shown in Fig. 14. As can be

observed in the figures, normalised column strengths ( $\chi_{\text{Exp+FE}}$ ) obtained from experiments and the FE parametric studies are generally above the column buckling curves, implying the conservative strength predictions obtained based on these standards. The accuracy and reliability of the standards for HSS cold-formed tubular columns were also examined, as illustrated in Sections 4.2 and 4.3.

## 4.2 Reliability analysis

The reliability of the design rules in EC3, AS4100 and AISC 360 standards were assessed by conducting a statistical analysis according to AISC 360 [5]. The reliability index ( $\beta$ ) for each design rule was calculated using Eq. (13) and the design rule is regarded as reliable if the reliability index is greater than 2.6 [5, 38]. Through this analysis, the differences in the reliability of different standards can be directly revealed through the calculated reliability index values for the standards [39-40]. The resistance factor ( $\phi$ ) of 1.0 is specified in EC3 while the value of 0.9 for  $\phi$  is provided in AS4100 and AISC 360 standards. The load combinations of  $1.35 \times \text{Dead load (DL)} + 1.5 \times \text{Live load (LL)}$  for EC3,  $1.2 \times \text{DL} + 1.5 \times \text{LL}$  for AS4100 and  $1.2 \times \text{DL} + 1.6 \times \text{LL}$  for AISC 360 were used in the estimation of  $\beta$ . The dead-to-live load ratio of 1/3 was adopted, as recommended in AISC 360 standard. The other statistical parameters  $M_m=1.10$ ,  $F_m=1.00$ ,  $V_m=0.10$  and  $V_F=0.05$  are the mean values and COV of the random variables related to the uncertainties in material properties and geometry of the cross-section [37, 39]. The parameter  $V_Q$  is the coefficient of variation of loading and equals to 0.19. The  $P_m$  and  $V_P$  are the mean and COV of the experimental/FE-to-predicted strengths ratios. The  $\xi$  was estimated to be 0.692, 0.710 and 0.675 for EC3, AS4100 and AISC 360 standards respectively.

$$\beta = \frac{\ln \left( \frac{M_m F_m P_m}{\xi \phi} \right)}{\sqrt{V_M^2 + V_F^2 + V_P^2 + V_Q^2}} \quad (13)$$

## 4.3 Evaluation of current design rules and suggestions for column buckling curve selection

A quantitative evaluation of the strength predictions based on EC3, AS4100 and AISC 360 was conducted. The  $\chi_{\text{EC3,c}}$  values were calculated based on column buckling curve c in EC3 using the material properties and geometric properties from experiments and parametric studies. The calculated  $\chi_{\text{EC3,c}}$  values were compared with the normalised column strengths ( $\chi_{\text{Exp+FE}}$ ) obtained from experiments and the FE parametric studies ( $\chi_{\text{Exp+FE}}$ ). The mean values for the ratios of  $\chi_{\text{Exp+FE}}$  over  $\chi_{\text{EC3,c}}$  are presented in Tables 5-8 together with the corresponding COV for SHS columns, RHS columns buckling about major and minor axes and CHS columns. As shown in the tables, the strengths predicted based on EC3 are lower than the strengths determined in experiments and FE parametric studies by 22-28% on average. The reliability index values for the columns with different

cross-sectional shapes and with steel grades of S700, S900 and S1100 are between 2.93 and 3.13 and greater than 2.6. In EC3, column buckling curves (a and b) providing higher  $\chi$  values are also given. Since conservative strength predictions were obtained using curve c, the accuracy and reliability of curves a and b to predict the strengths of the cold-formed SHS, RHS and CHS columns with steel grades of S700, S900 and S1100 were also evaluated, as shown in Tables 5-8. Based on the evaluation, suggestions on the column buckling curve selection were also provided in the tables for the columns. As can be seen in the tables, column buckling curve b can be applied to more accurately predict the strengths of the columns.

The comparisons between the strength predictions based on the AS4100 ( $\chi_{AS,\alpha_b=-0.5}$ ) and the column strengths obtained from experiments and FE parametric studies are presented in Tables 5-8 for SHS columns, RHS columns buckling about major and minor axes and CHS columns. The strengths of the columns were underestimated using the buckling curve for the  $\alpha_b$  value of -0.5 by 7-9% on average. The design rule from AS4100 is reliable for the columns since the  $\beta$  values are greater than 2.6. In AS4100, the buckling curve based on the  $\alpha_b$  value of -1 provides higher  $\chi$  values and was also used to predict the strengths of the columns ( $\chi_{AS,\alpha_b=-1}$ ). For SHS, RHS and CHS columns with S700, S900 and S1100 steel grades, the mean values of  $\chi_{Exp+FE}/\chi_{AS,\alpha_b=-1}$  are about 1.00-1.02 with the COV of 0.02-0.04, as shown in Tables 5-8. Although the predictions based on the value of -1 for  $\alpha_b$  are more accurate and less scattered than those estimated based on the  $\alpha_b$  value of -0.5, the reliability index values for strength predictions using the value of -1 for  $\alpha_b$  are below the required value of 2.6. Tables 5-8 also present the quantitative evaluation of the strength predictions using the column buckling curve from AISC 360. The evaluation shows that the AISC 360 provides conservative strength predictions for the SHS columns, RHS columns buckling about major and minor axes and CHS columns. The mean values of  $\chi_{Exp+FE}/\chi_{AISC}$  are about 1.07-1.11 with the COV of 0.02-0.05. The design rule from AISC 360 also satisfies the reliability requirement with the  $\beta$  values ranging from 2.97 to 3.15. Since a single column buckling curve is provided in AISC 360 standard, no suggestion on column curve selection was made.

#### 4.4 Proposed column buckling curve expression

The evaluation of the design rules in standards shows that these column buckling curves provide conservative predictions for the strength of SHS, RHS and CHS columns formed using S700, S900 and S1100 steel, as discussed in Section 4.3. The applicability of alternative column buckling curves given in the European and Australian standards was assessed. However, the conservative strength predictions by about 13-18% were also obtained using column buckling curves b from European standard based on discrete values for  $\alpha$  while the alternative column buckling curve based on the  $\alpha_b$  of -1 from Australian standard is unreliable for strength predictions. In order to accurately predict the

strengths of the columns, an analytical expression considering the increment of normalised column strengths with increasing steel grades is proposed in this section and can be used more conveniently for cold-formed SHS, RHS and CHS columns with different steel grades.

The Ayron-Perry equation given as Eq. (14) [41] was adopted and employed as the basic formula for the proposed column curve because the equation is versatile for establishing column curves by varying the imperfection parameter  $\eta$  which can be used to account for the effects of geometric imperfection and residual stress on the strength of any column. The value of  $\eta$  can be calculated using Eq. (15) [42-43]. The Ayron-Perry equation was used to establish column buckling curves in Eurocode 3 and can also be applied to closely model the Structural Stability Research Council (SSRC) column strength curves [9] which have been used as the column buckling curves in AS4100 and AISC 360 [42-44].

$$\chi = \frac{1+\eta+\bar{\lambda}^2}{2\bar{\lambda}^2} - \frac{1}{2\bar{\lambda}^2} \sqrt{[1 + \eta + \bar{\lambda}^2]^2 - 4\bar{\lambda}^2}, \text{ but } \chi \leq 1 \quad (14)$$

$$\eta = \alpha(\bar{\lambda} - 0.2) \quad (15)$$

In order to incorporate the influence of yield strength in estimating the column strengths, a term  $\varepsilon$  defined in Eq. (16) is introduced to Eq. (15) which is subsequently modified into Eq. (17). In Eq. (16), the number 235 represents the nominal yield strength of the reference steel grade S235. The value of 0.49 for  $\alpha$  obtained based on experimental and numerical results for conventional strength steel columns [3, 43] is also applied in Eq. (17).

$$\varepsilon = (235/f_y)^{0.5} \quad (16)$$

$$\eta = \alpha * (\bar{\lambda} * \varepsilon - 0.2) \quad (17)$$

The reduction factor  $\chi_{\text{pro}}$  calculated from Eqs. (14), (16) and (17) for varying  $\bar{\lambda}$  is plotted in Figs. 15-18 in comparison with the normalised column strengths obtained from available experimental data and FE parametric studies for SHS, RHS and CHS steel columns. As can be observed in Figs. 15-18, the column buckling curves obtained using Eqs. (14), (16) and (17) closely match the experimental and FE data and provide the lower bound for the normalised strengths of columns with each steel grade. The longer plateau with  $\chi$  equals to unity obtained for the proposed column curves also agree well with the experimental and FE results for columns with low member slenderness. The limiting member slenderness value for the plateau tends to increase with increasing steel grade, since the normalised column strengths increase with the steel grade.

The average ratios  $\chi_{\text{Exp+FE}}/\chi_{\text{pro}}$  for S700-S1100 columns with different cross-sections were also calculated, as shown in Tables. 5-8. As can be seen in the tables, the average ratios  $\chi_{\text{Exp+FE}}/\chi_{\text{pro}}$  are between 1.05 and 1.08 with the COV ranging from 0.01 to 0.03. Thus, the strength predictions using the proposed column buckling curve expression are conservative on an average basis and in good consistency with the results of experiments and FE parametric studies. Reliability analysis was also carried out for the proposed column buckling curve expression and the load combination of  $1.35 \times \text{DL} + 1.5 \times \text{LL}$  was used. The reliability index varies between 2.79 and 2.90 when a resistance factor of 0.9 is used. Therefore, the proposed column buckling curve expression can be used to obtain accurate and reliable strength predictions for the cold-formed HSS columns. Comparing with existing design rules in standards for cold-formed tubular columns, the proposed column buckling curve expression provides more accurate strength predictions especially for columns with higher steel grades while has lower  $\beta$  values than the design rule in AISC 360 [5], as shown in Tables 5-8.

## 5. Conclusions

Structural performance of cold-formed high strength steel SHS, RHS and CHS columns was investigated numerically. A FE model was developed and validated against experimental results. Extensive parametric studies of SHS, RHS and CHS columns with a wide range of cross-sectional dimensions, member slenderness values and steel grades of S700, S900 and S1100 were carried out using the validated FE model. Effect of global geometric imperfections on the column strengths was investigated and found to reduce with increasing steel grade from S700 to S1100 for SHS, RHS and CHS columns. Comparing with the S700 columns, columns with steel grades of S900 and S1100 respectively showed higher normalised column strengths by 0.5-4.2 and 1.0-7.4% since the reduction effect of global geometric imperfection and residual stress on the column strengths became less severe. In addition, the effect of  $f_u/f_y$  ratio on the normalised column strengths was found to be quite limited.

Based on the experimental data in literature and the FE parametric studies results obtained in this study, the applicability of design rules in European, Australian and American standards to the cold-formed SHS, RHS and CHS columns with steel grades of S700, S900 and S1100 was examined. The design rules in these standards provide quite conservative and reliable predictions of column strengths. Suggestions on the selection of column buckling curve for predicting the column strengths were discussed. In addition, a new column buckling curve expression taking into account the improved normalised column strengths with increasing steel grade was proposed and found to provide accurate and reliable strength predictions for the cold-formed SHS, RHS and CHS columns with steel grades of S700, S900 and S1100.

## Acknowledgement

The authors are grateful for the support from the Chinese National Engineering Research Centre for Steel Construction (Hong Kong Branch) at The Hong Kong Polytechnic University. The financial support from The Hong Kong Polytechnic University (PolyU: 1-ZE50/G-YBUU) is also gratefully acknowledged.

## References

- [1] Uy, B. 2005. Composite steel-concrete beams and columns fabricated with high strength steel (HSS) plate. In proceedings of *4th European Conference on Steel and Composite Structures*, Germany. p.4.2-23-4.2-30.
- [2] Gogou, E. 2012. Use of high strength steel grades for economical bridge design. Master thesis. Faculty of Civil Engineering and Geosciences, Delft University of Technology.
- [3] EN 1993-1-1, 2005. *Eurocode 3: Design of steel structures - Part 1-1: General rules and rules for buildings*. Brussels: European Committee for Standardization.
- [4] EN1993-1-12, 2007. *Eurocode 3: Design of steel structures - Part 1-12: Additional rules for the extension of EN1993 up to steel grades S700*. Brussels: European Committee for Standardization.
- [5] ANSI/AISC 360-16, 2016. *Specification for structural steel buildings*. AISC, Chicago.
- [6] AS4100, 1998. *Australian Standard. Steel structures*. NSW, Australia: Standards Australia.
- [7] AS4100-A1, 2012. *Australian Standard. Amendment No.1 to AS4100-1998 steel structures*. NSW, Australia: Standards Australia.
- [8] Sfintesco, D. 1970. Fondement expérimental des courbes européennes de flambement. *Construetion Métallique*, No. 3, 5-12. (in French)
- [9] Ziemian, R.D. 2010. *Guide to stability design criteria for metal structures*. 5<sup>th</sup> Edition, Wiley, Hoboken, New Jersey.
- [10] Somodi, B. and Kövesdi, B. 2017. Residual stress measurements on cold-formed HSS hollow section columns. *Journal of Constructional Steel Research*, 128, 706-720.
- [11] Ma, J.L., Chan, T.M. and Young, B. 2017. Tests on high-strength steel hollow sections: a review. *Proceedings of the Institution of Civil Engineers – Structures and Buildings*, 170 (SB9), 621-630.

469 [12] Chan, T.M., Zhao, X.L. and Young, B. 2015. Cross-section classification for cold-formed and  
470 built-up high strength carbon and stainless steel tubes under compression. *Journal of Constructional*  
471 *Steel Research*, 106, 289-295.

472 [13] Shi, G., Jiang, X., Zhou, E.J., Chan, T.M. and Zhang, Y. 2014. Experimental study on column  
473 buckling of 420 MPa high strength steel welded circular tubes. *Journal of Constructional Steel*  
474 *Research*, 100, 71-81.

475 [14] Wang, J., Afshan, S., Schillo, N., Theofanous, M., Feldmann, M. and Gardner, L. 2017. Material  
476 properties and compressive local buckling response of high strength steel square and rectangular  
477 hollow sections. *Engineering Structures*, 130, 297-315.

478 [15] Rasmussen, K.J.R. and Hancock, G.J. 1992. Plate slenderness limits for high strength steel  
479 sections. *Journal of Constructional Steel Research*, 23, 73-96.

480 [16] Rasmussen, K.J.R. and Hancock, G.J. 1995. Tests of high strength steel columns. *Journal of*  
481 *Constructional Steel Research*, 34, 27-52.

482 [17] Somodi, B. and Kövesdi, B. 2017. Flexural buckling resistance of cold-formed HSS hollow  
483 section members. *Journal of Constructional Steel Research*, 128, 179-192.

484 [18] Dundu, M. and Chabalala, V. 2014. Cold-formed circular hollow sections under axial  
485 compression. *Proceedings of the 1st International Conference on the Construction Materials and*  
486 *Structures (ICCMATS-1)*, ISO Press, Amsterdam, The Netherlands. p. 1148-1154.

487 [19] Ma, J.L. 2016. Behaviour and design of cold-formed high strength steel tubular members. Ph.D.  
488 thesis. Department of Civil Engineering, The University of Hong Kong.

489 [20] Javidan, F., Heidarpour, A., Zhao, X.L. and Minkinen, J. 2016. Application of high strength and  
490 ultra-high strength steel tubes in long hybrid compressive members: experimental and numerical  
491 investigation. *Thin-walled Structures*, 102, 273-285.

492 [21] ABAQUS [Computer software] version 6.12 (2012). Dassault Systèmes, Providence, RI.

493 [22] Chan, T.M. and Gardner, L. 2009. Flexural buckling of elliptical hollow section columns.  
494 *Journal of Structural Engineering*, 135, 546-557.

495 [23] Fang, H. and Chan, T.M. 2018. Axial compressive strength of welded S460 steel columns at  
496 elevated temperatures. *Thin-walled Structures*, 129, 213-224.

497 [24] Chan, T.M. and Gardner, L. 2009. Compressive resistance of hot-rolled elliptical hollow  
498 sections. *Engineering Structures*, 30, 522-532.



499 [25] Ma, J.L., Chan, T.M. and Young, B. 2015. Material properties and residual stresses of cold-  
500 formed high strength steel hollow sections. *Journal of Constructional Steel Research*, 109, 152-165.

501 [26] Cruise, R.B. and Gardner, L. 2008. Strength enhancements induced during cold forming of  
502 stainless steel sections. *Journal of Constructional Steel Research*, 64, 1310-1316.

503 [27] Zhao, O., Rossi, B., Gardner, L. and Young, B. 2015. Behaviour of structural stainless steel  
504 cross-sections under combined loading – Part II: Numerical modelling and design  
505 approach. *Engineering Structures*, 89, 247-259.

506 [28] Ma, J.L., Chan, T.M. and Young, B. 2016. Experimental investigation on stub-column behaviour  
507 of cold-formed high strength steel tubular sections. *Journal of Structural Engineering*, 142, 04015174.

508 [29] Ma, J.L., Chan, T.M. and Young, B. 2017. Design of cold-formed high strength steel tubular  
509 beams. *Engineering Structures*, 151, 432-443.

510 [30] Rasmussen, K.R. and Hancock, G.J. 1993. Design of cold-formed stainless steel tubular members.  
511 I: Columns. *Journal of Structural Engineering*, 119, 2349-2367.

512 [31] Theofanous, M. and Gardner, L. 2009. Testing and numerical modelling of lean duplex stainless  
513 steel hollow section columns. *Engineering Structures*, 31, 3047-3058.

514 [32] Tide, R.H.R. 1985. Reasonable column design equations. Proceedings of *the Annual Technical*  
515 *Session of Structural Stability Research Council*, Lehigh University, Bethlehem, Pennsylvania. p.47-  
516 55.

517 [33] Tide, R.H.R. 2001. A technical note: Derivation of the LRFD Column Design Equations.  
518 *Engineering Journal*, 38, 137-139.

519 [34] Beedle, L.S. 1991. *Stability of metal structures: A world view*. Structural Stability Council,  
520 Lehigh University, Bethlehem, Pennsylvania.

521 [35] ANSI/AISI S100-16, 2016. *North American specification for the design of cold-formed steel*  
522 *structural members*. AISI, Washington, DC.

523 [36] AS4600, 2005. *Australian Standard. Cold-formed steel structures*. Sydney, Australia: Standards  
524 Australia.

525 [37] Ma, J.L., Chan, T.M. and Young, B. 2018. Design of cold-formed high strength steel tubular stub  
526 columns. *Journal of Structural Engineering*, 144(6), 04018063.

- 527 [38] Wang, J. and Gardner, L. 2017. Flexural buckling of hot-finished high-strength steel SHS and  
528 RHS columns. *Journal of Structural Engineering*, 143 (6): 04017028.
- 529 [39] Pham, L., Holmes, D. and Yang, J. 1992. Reliability analysis of Australian communication lattice  
530 tower. *Journal of Constructional Steel Research*, 23, 255-272.
- 531 [40] Zhao, X.L., Riadh, A.M. and Kiew, K.P. 1999. Longitudinal fillet welds in thin-walled C450  
532 RHS members. *Journal of Structural Engineering*, 125, 821-828.
- 533 [41] Ayrton, W.E. and Perry, J. 1886. On struts. *The Engineer*, 62, 464-465.
- 534 [42] Trahair, N.S. and Bradford, M.A. 1998. *The behaviour and design of steel structures to AS4100*.  
535 3<sup>th</sup> Edition, E & FN Spon, London.
- 536 [43] Rondal, J. and Maquoi, R. 1979. Formulation d'Ayrton\_Perry pour le flambement des barres  
537 métalliques. *Construction Métallique*, No. 4, 41-53. (in French)
- 538 [44] Maquoi, R. 1982. Some improvements to the buckling design of centrally loaded columns.  
539 *Proceeding of the annual meeting*, Structural Stability Research Council.

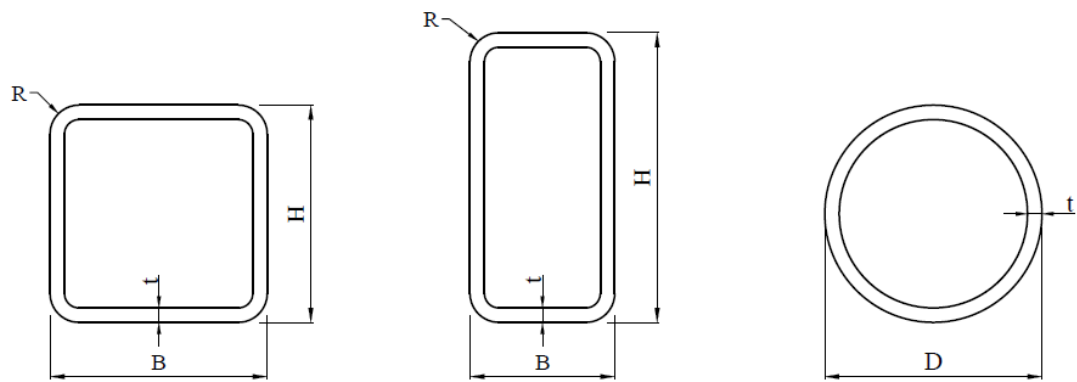


**Figure 1.** Definition of symbols in SHS, RHS and CHS.



**Figure 2.** The mesh and support condition for CF7-R150\*8\_1B column.

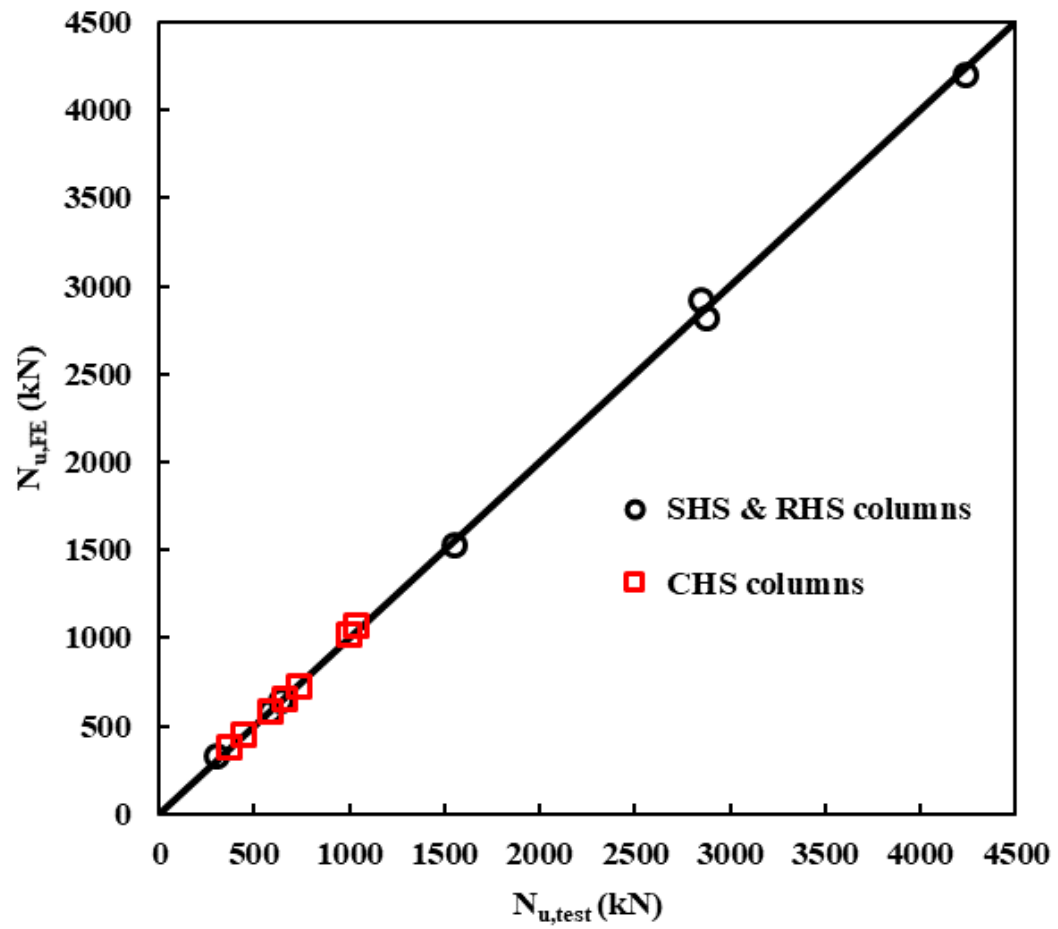


**Figure 3.** Comparison of the column strengths obtained from FE modelling and experiments [17-20] for SHS, RHS and CHS columns.

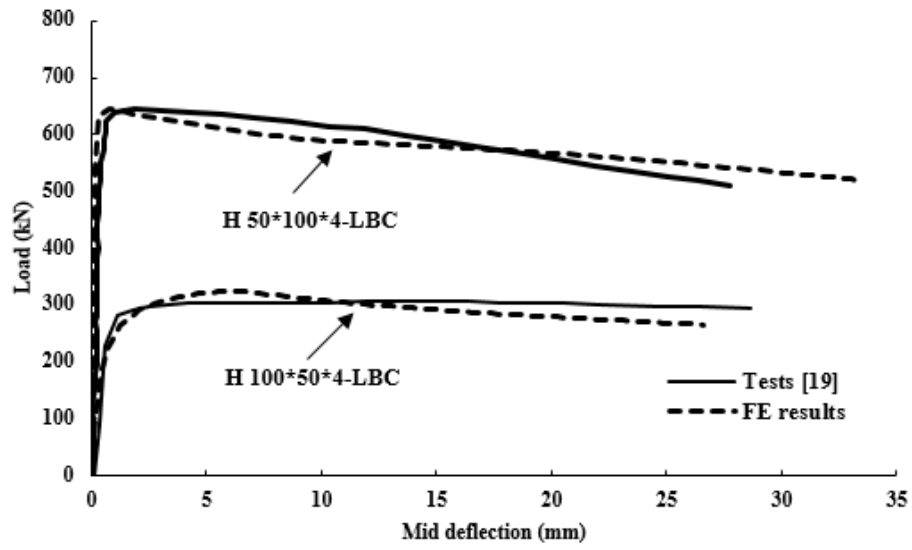


**Figure 4.** Comparison between the load-mid deflection curves obtained from experiments and FE modelling for H 50\*100\*4-LBC [19] and H 100\*50\*4-LBC [19] columns.

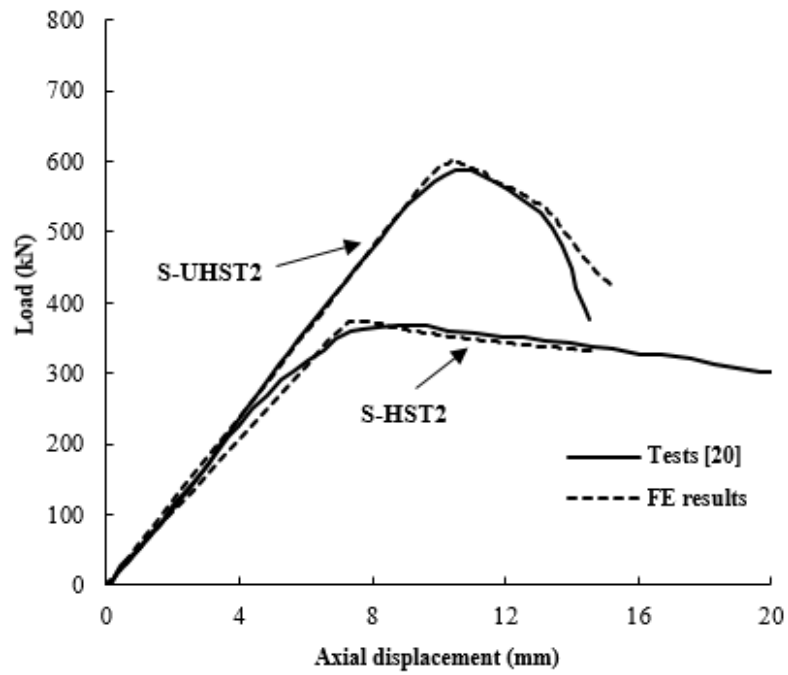


**Figure 5.** Comparison between the load-axial displacement curves obtained from experiments and FE modelling for S-HST2 [20] and S-UHST2 [20] columns.



**Figure 6.** Failure mode in the experiment and in the numerical model for the H 50\*100\*4-LBC [19] column.





**Figure 7.** Failure mode in the experiment and in the numerical model for the S-HST2 [20] column.

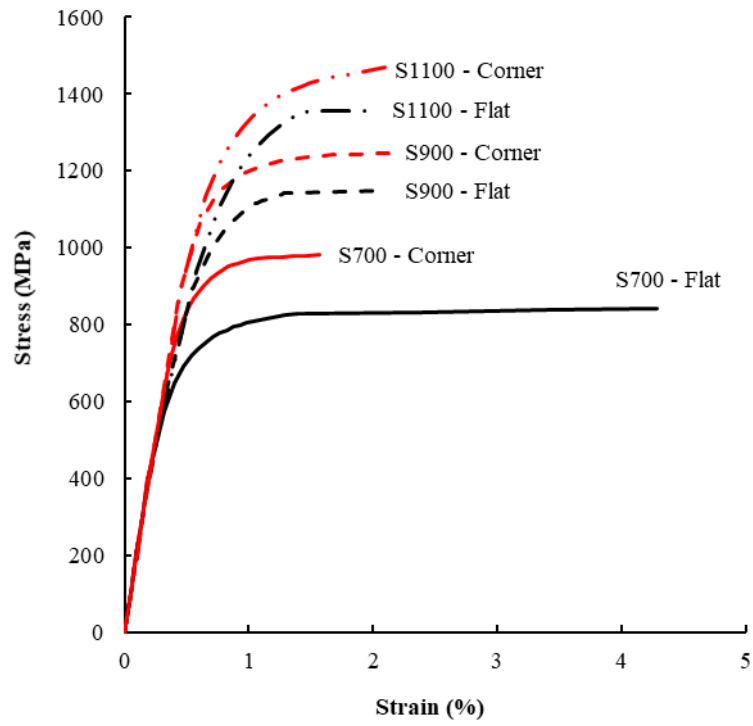
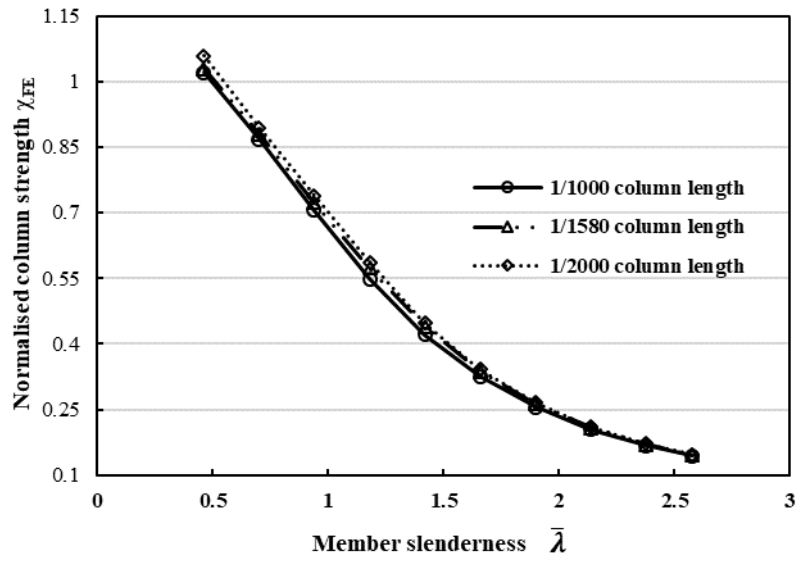
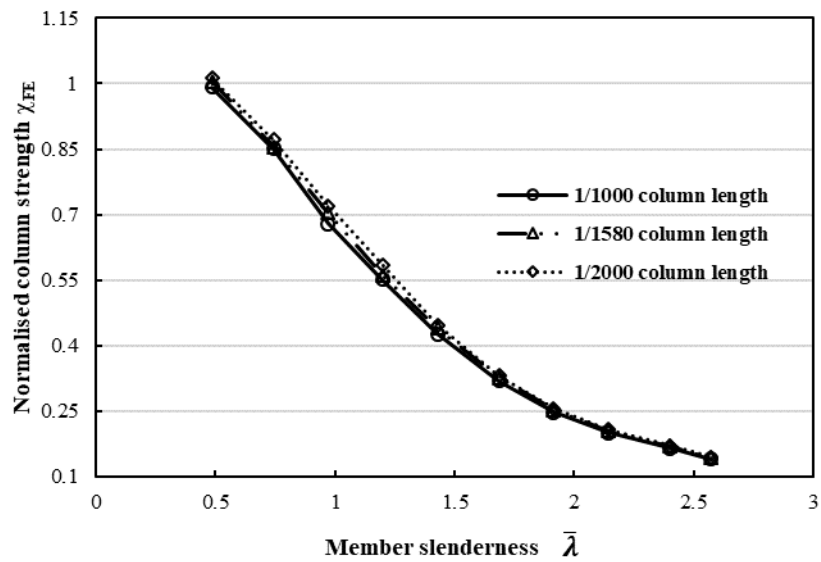


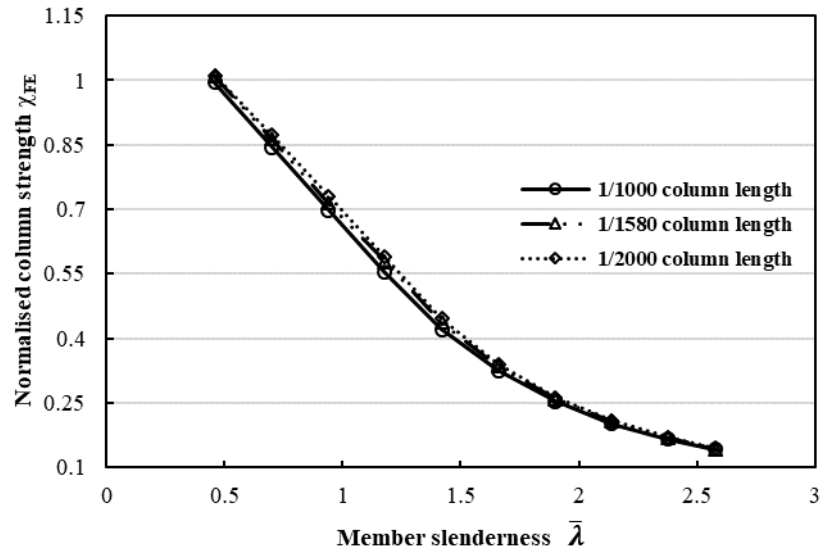
**Figure 8.** Typical stress-strain curves obtained for flat and corner materials using the model in [25].



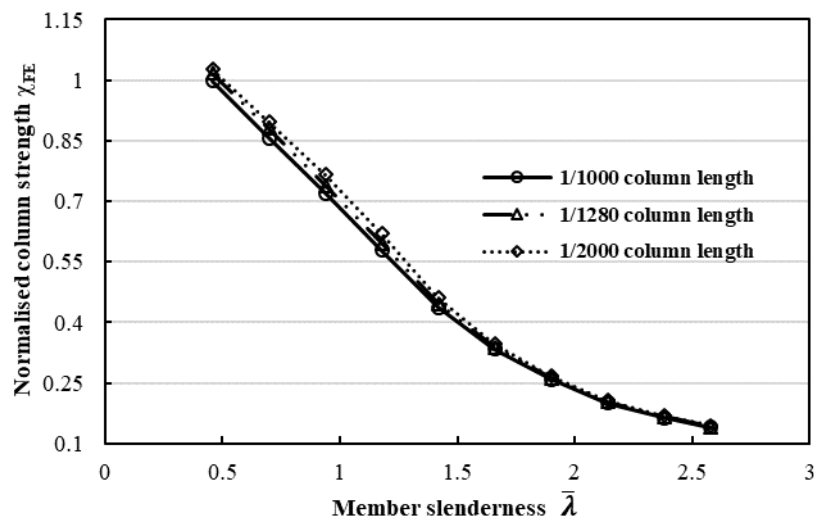
(a) SHS



(b) RHS buckling about major axis

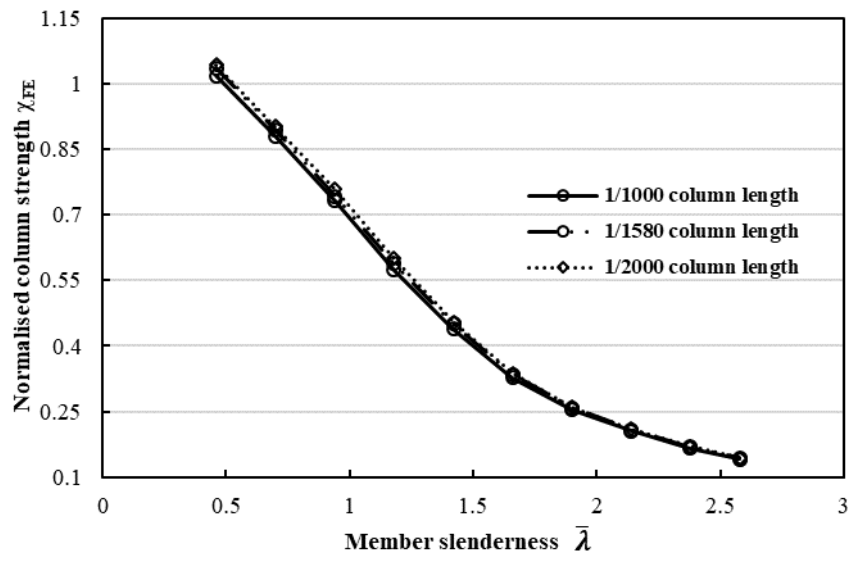


(c) RHS buckling about minor axis

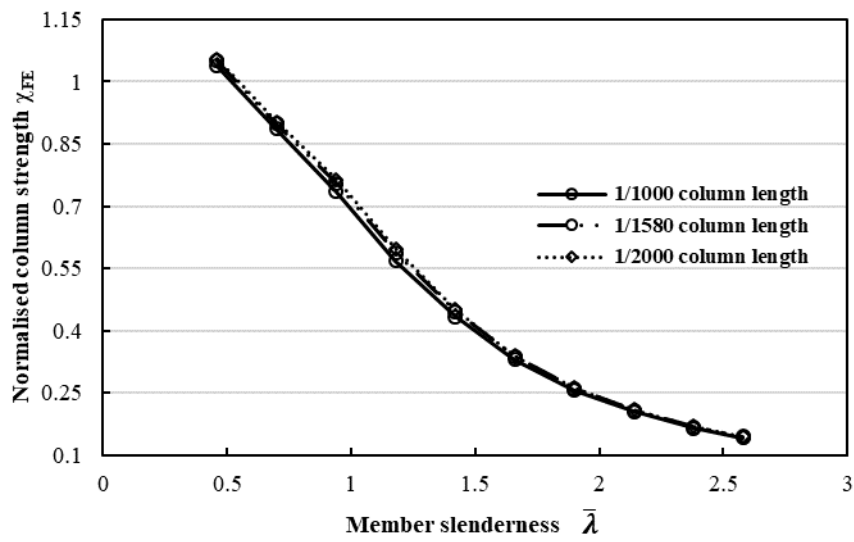


(d) CHS

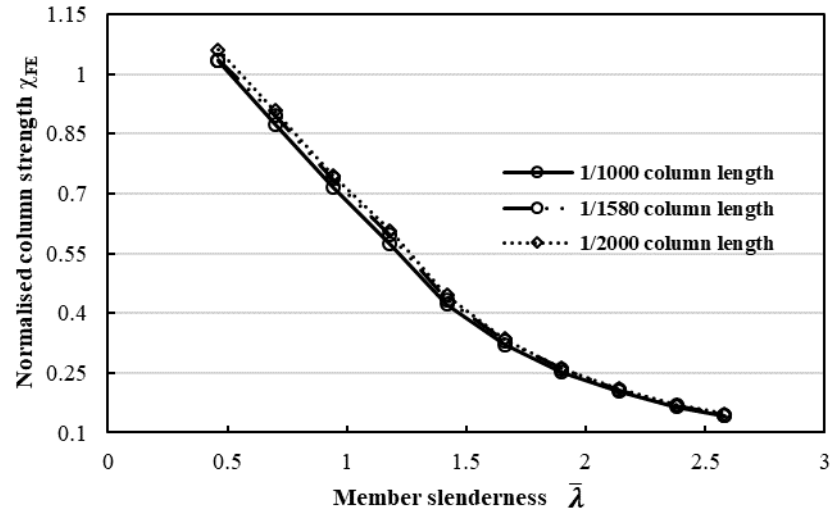
**Figure 9.** Comparisons of FE results for S700 columns with different global geometric imperfection magnitudes.



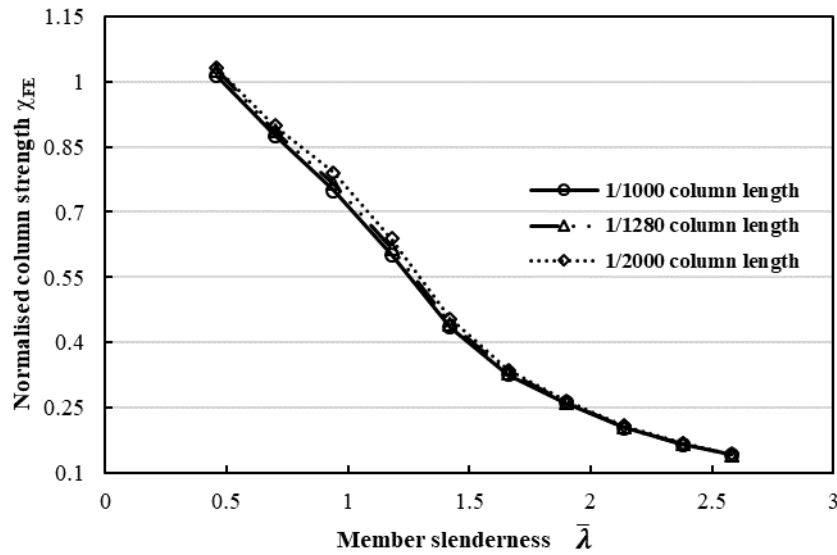
(a) SHS



(b) RHS buckling about major axis

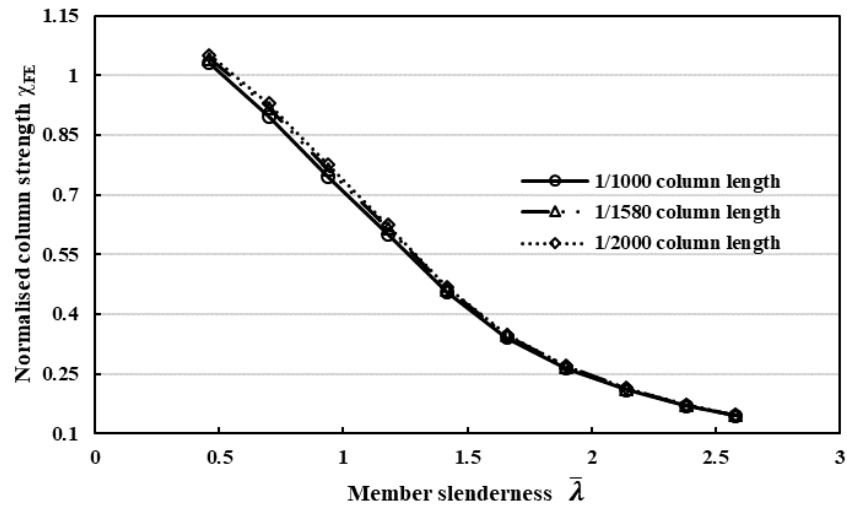


(c) RHS buckling about minor axis

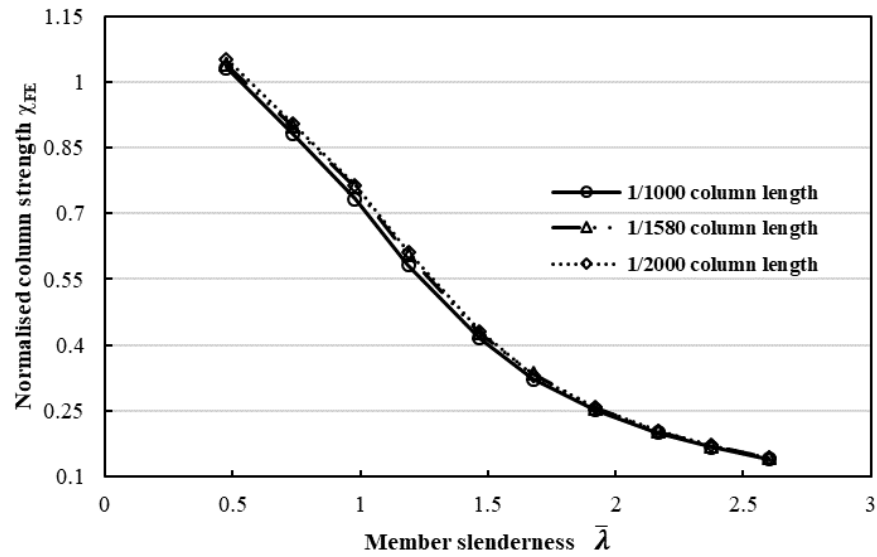


(d) CHS

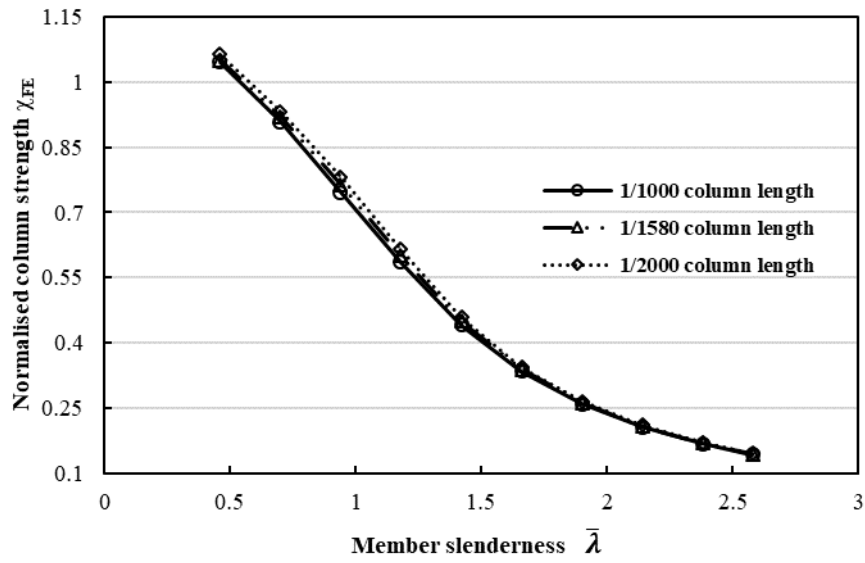
**Figure 10.** Comparisons of FE results for S900 columns with different global geometric imperfection magnitudes.



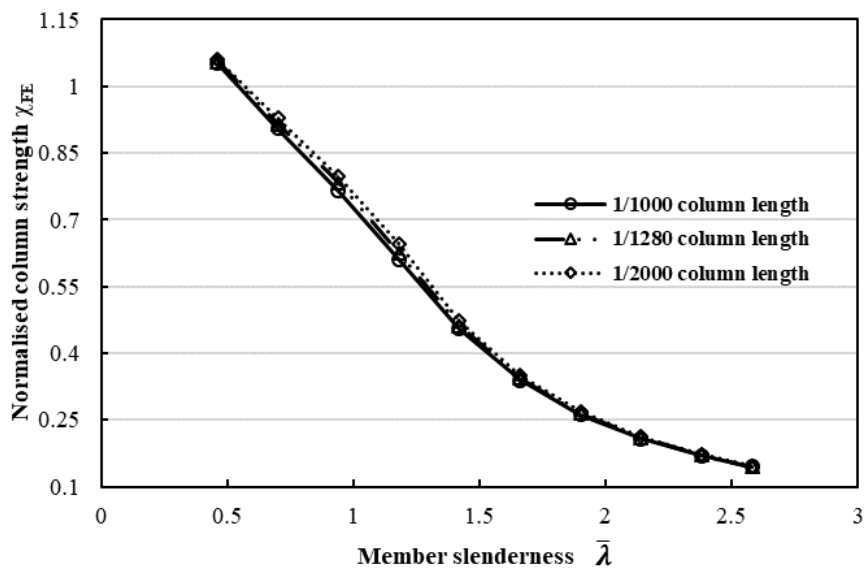
(a) SHS



(b) RHS buckling about major axis



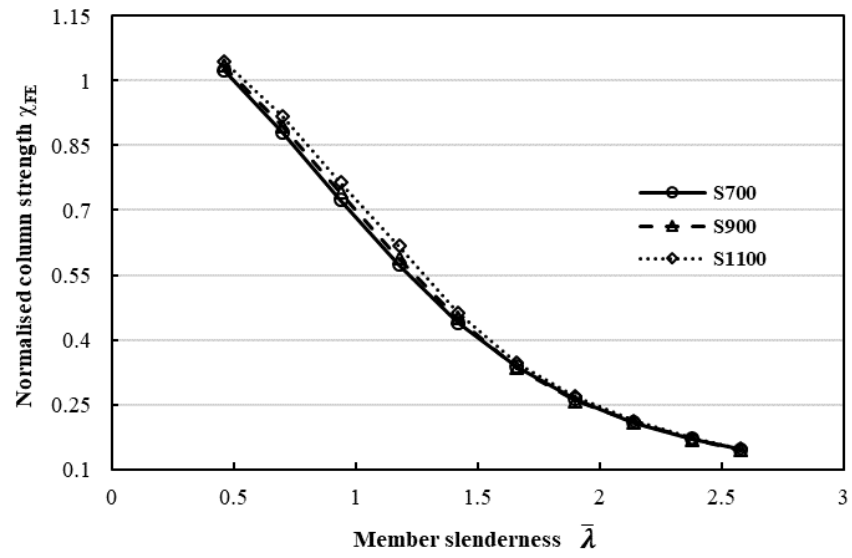
(c) RHS buckling about minor axis



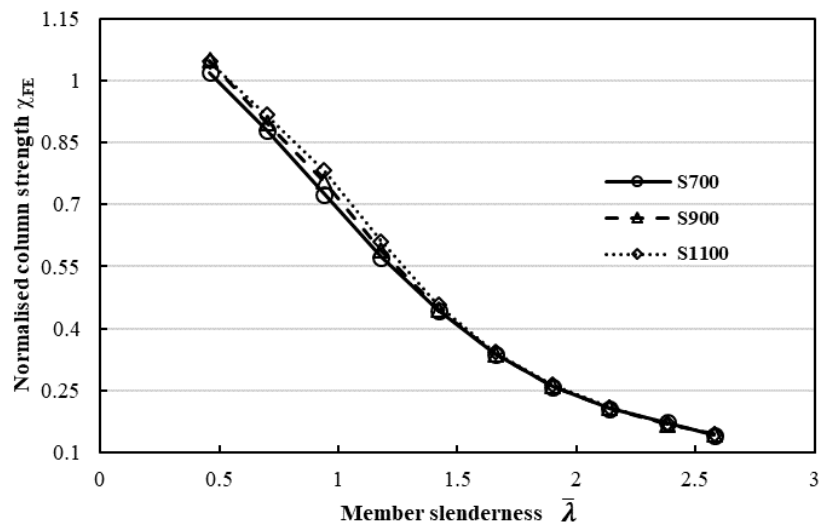
(d) CHS

**Figure 11.** Comparisons of FE results for S1100 columns with different global geometric imperfection magnitudes.

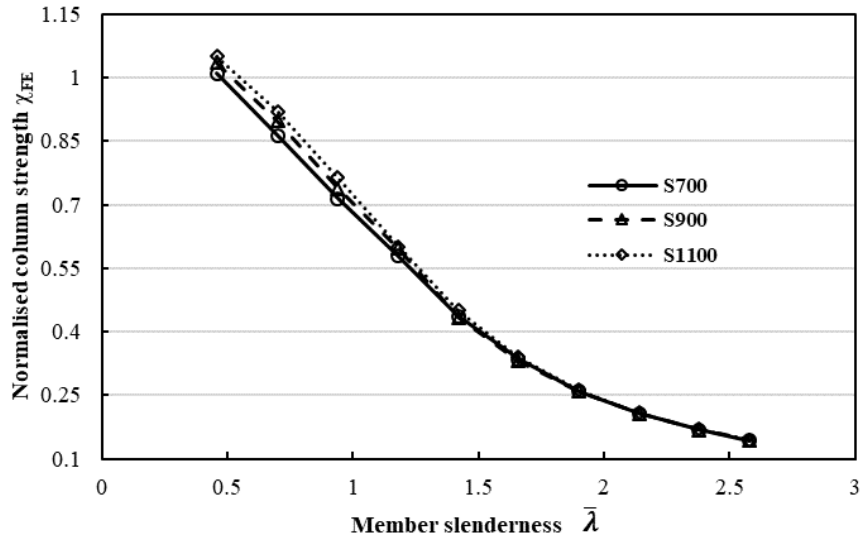




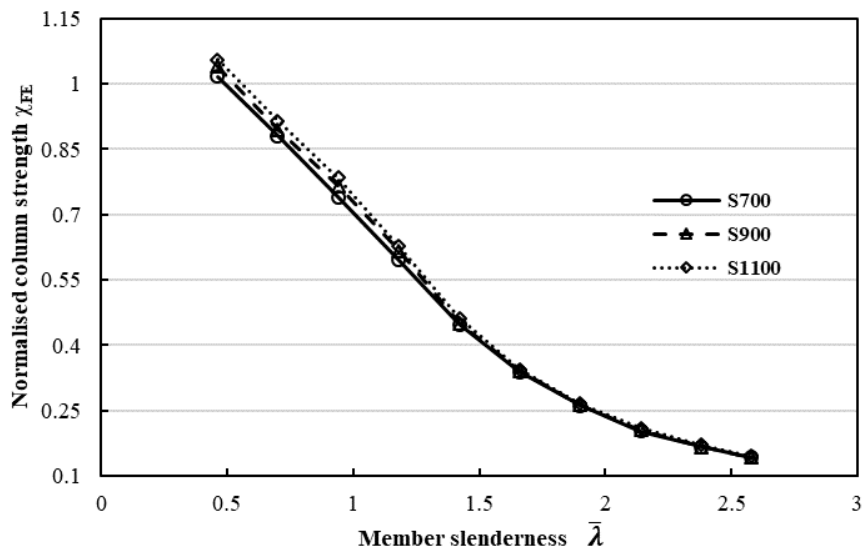
(a) SHS



(b) RHS buckling about major axis

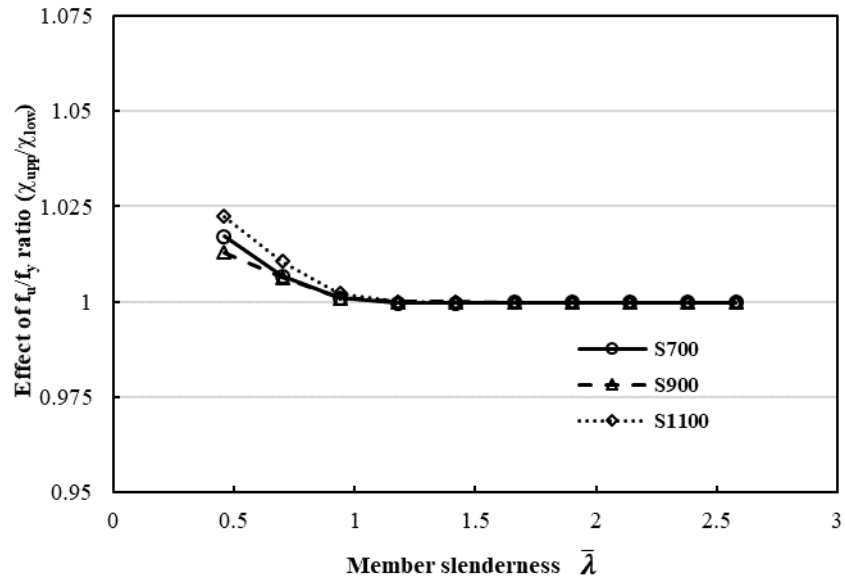


(c) RHS buckling about minor axis

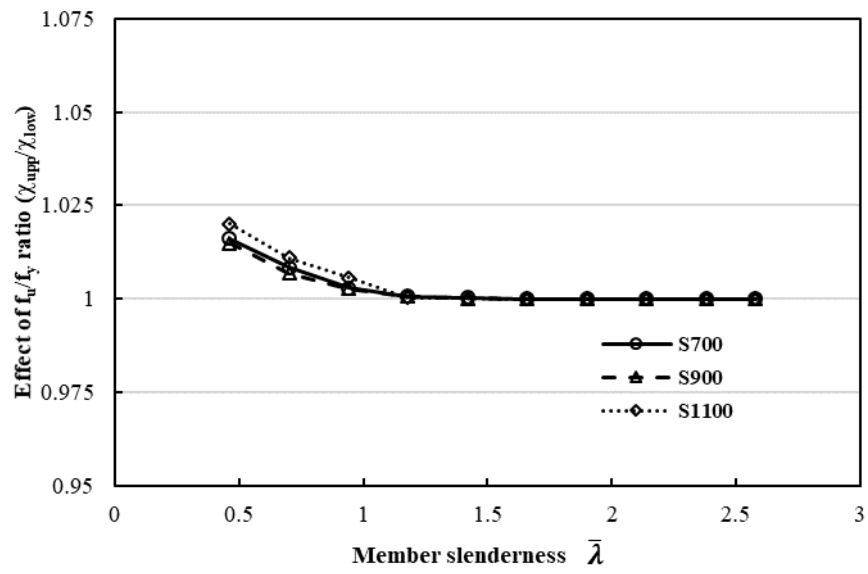


(d) CHS

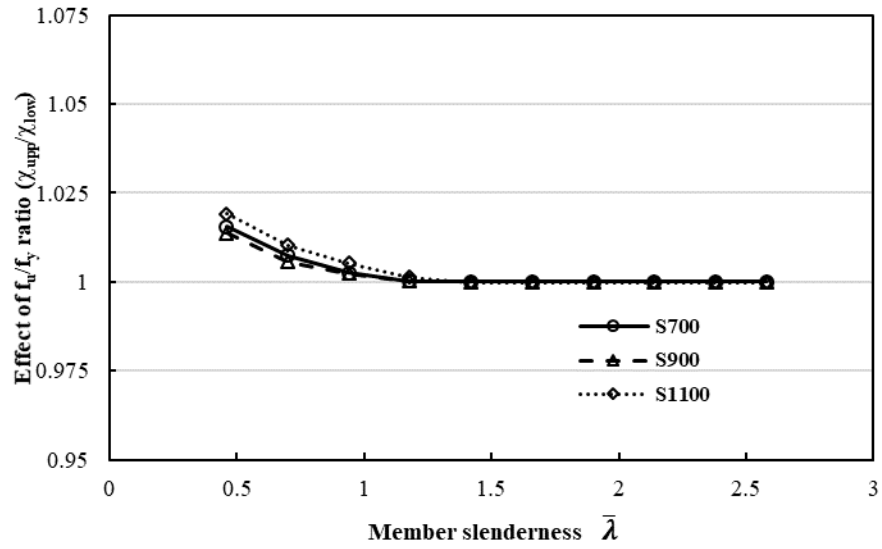
**Figure 12.** Comparisons of FE results for SHS, RHS and CHS columns with steel grades of S700, S900 and S1100.



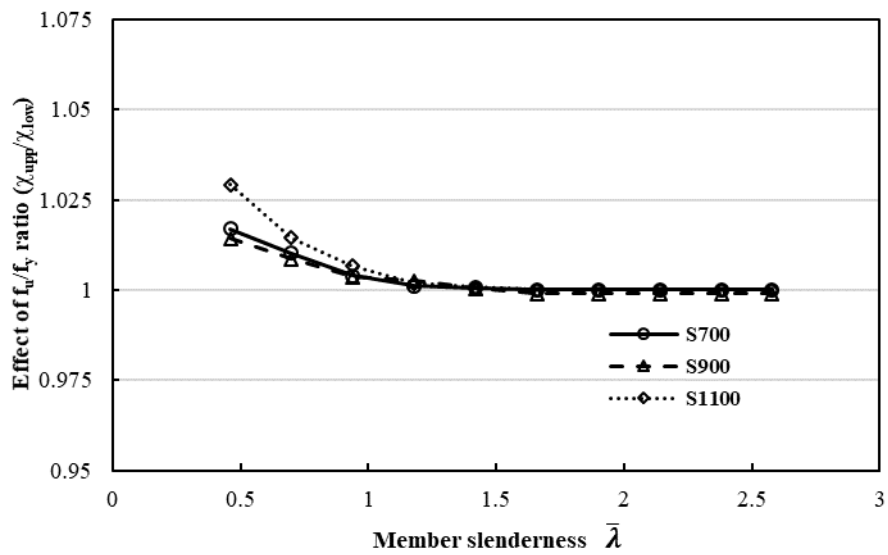
(a) SHS



(b) RHS buckling about major axis

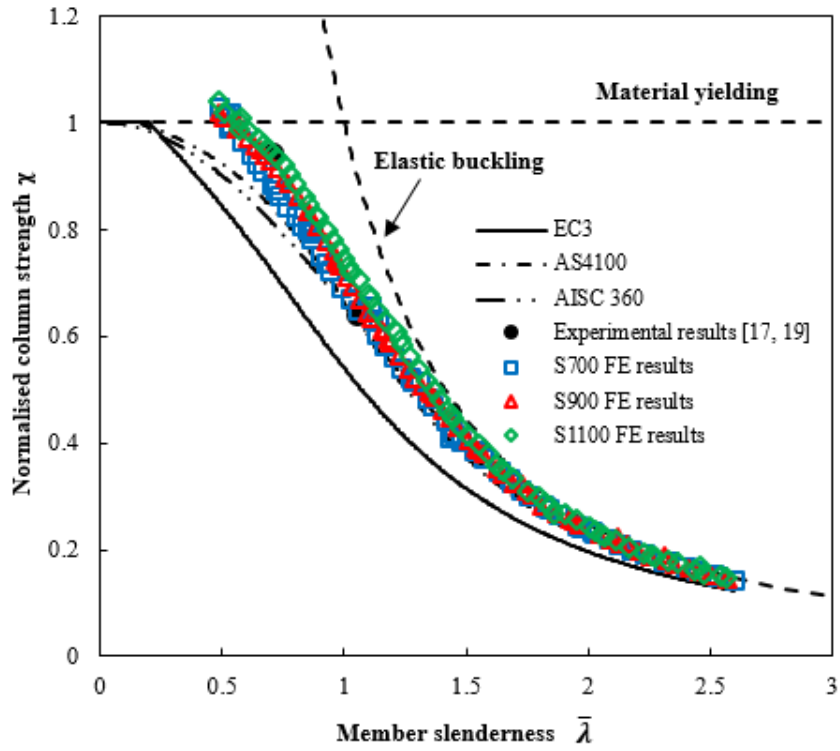


(c) RHS buckling about minor axis

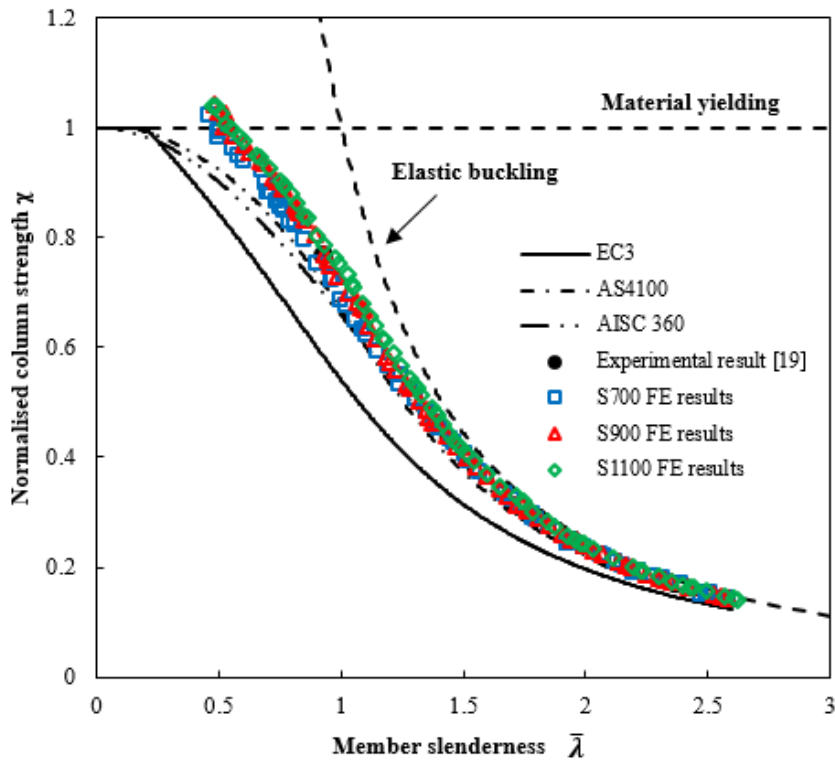


(d) CHS

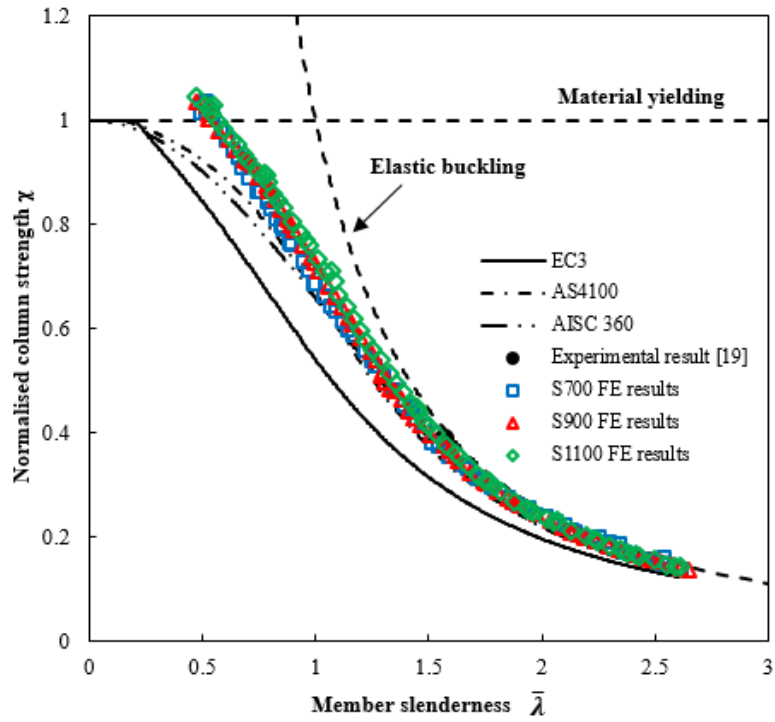
**Figure 13.** Effect of  $f_u/f_y$  ratio on the strengths of (a) SHS columns; (b) RHS columns buckling about major axis; (c) RHS columns buckling about minor axis and (d) CHS columns.



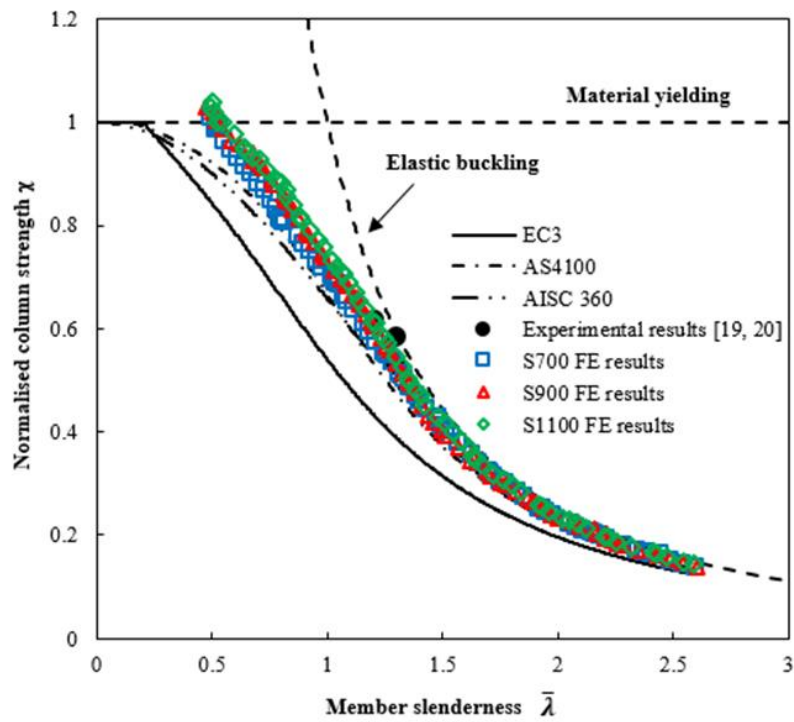
(a) SHS



(b) RHS buckling about major axis

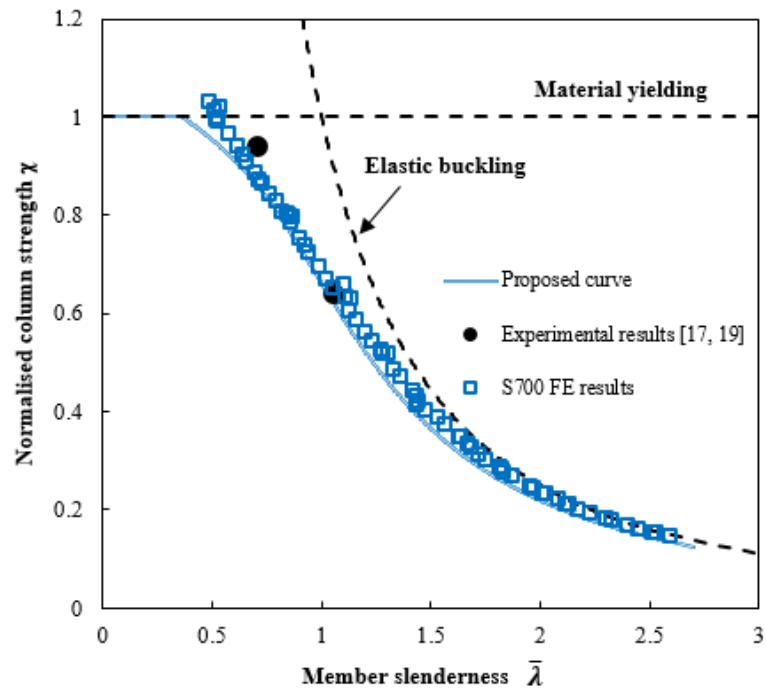


(c) RHS buckling about minor axis

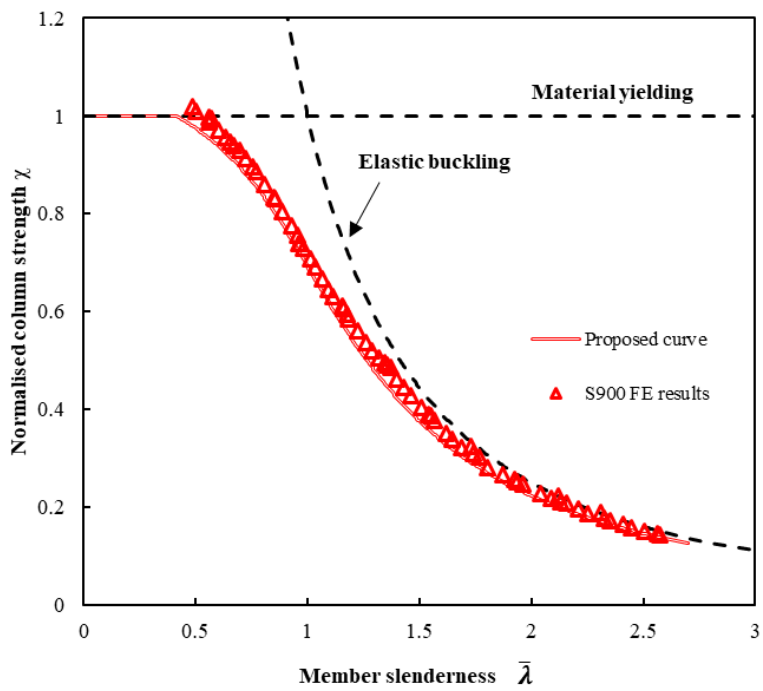


(d) CHS

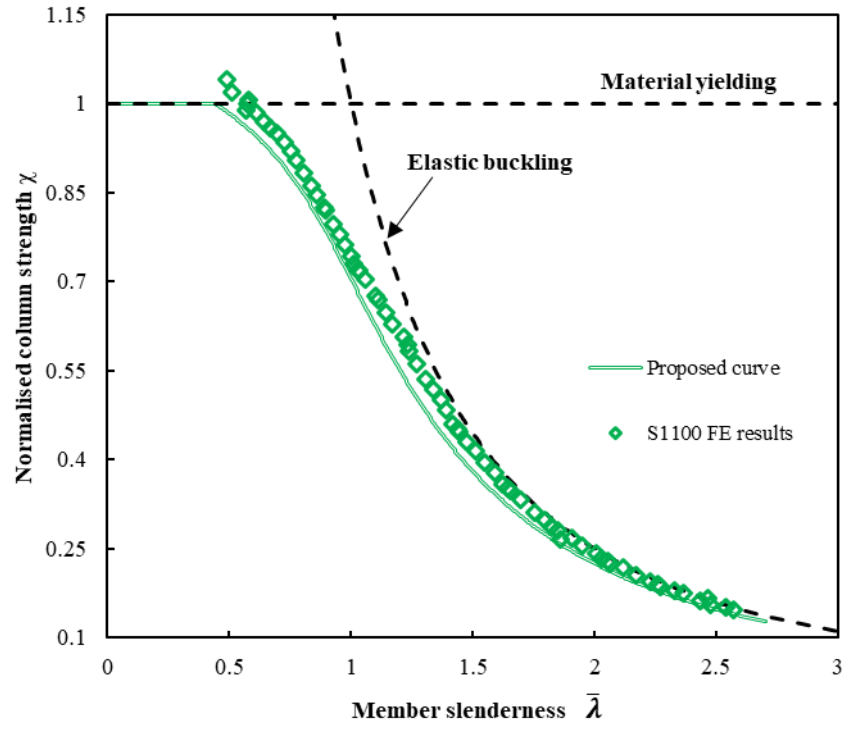
**Figure 14.** Column buckling curves and normalised column strengths from experiments and parametric studies.



(a)



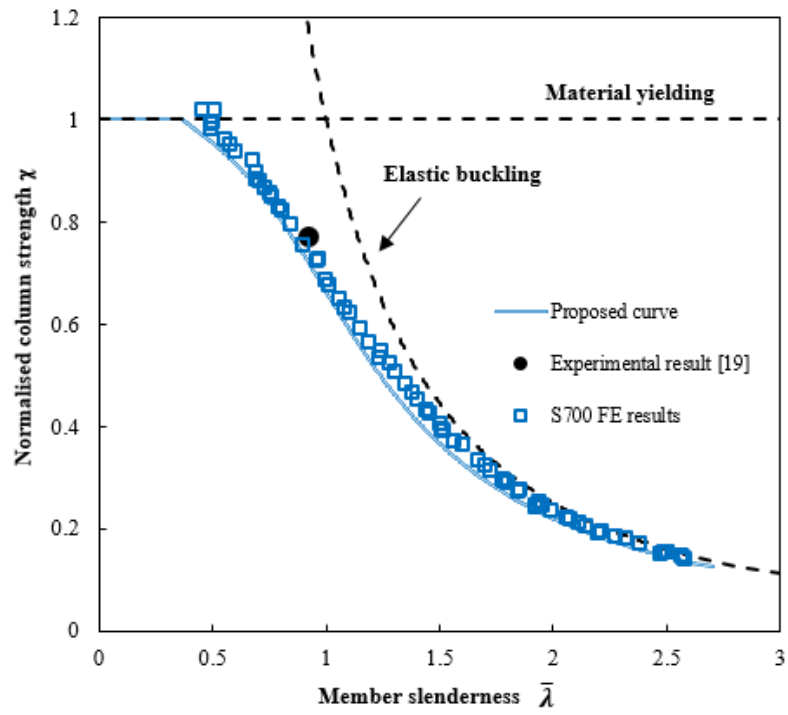
(b)



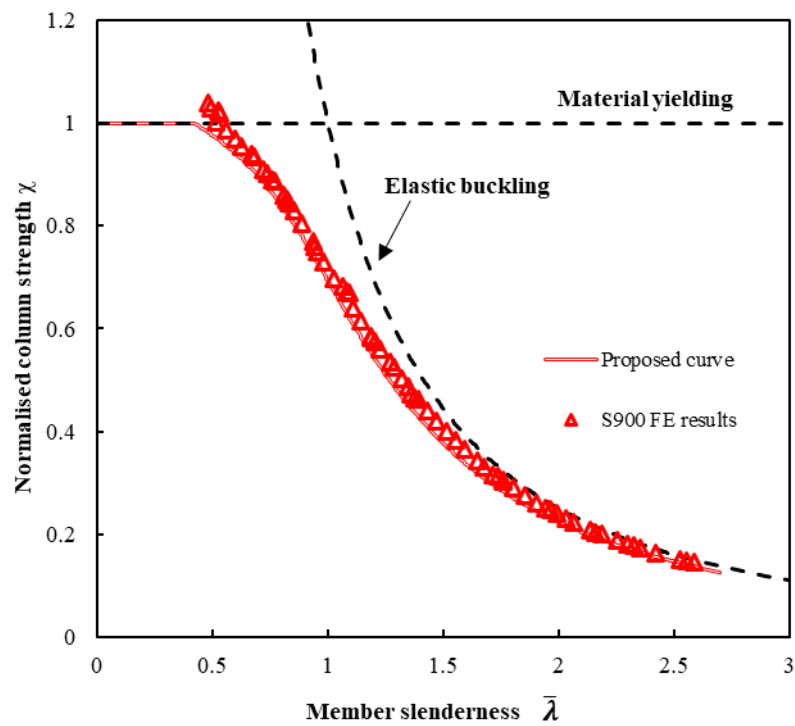
(c)

**Figure 15.** Comparison of the proposed column buckling curve with experimental and FE results for SHS columns with steel grade of (a) S700; (b) S900 and (c) S1100.

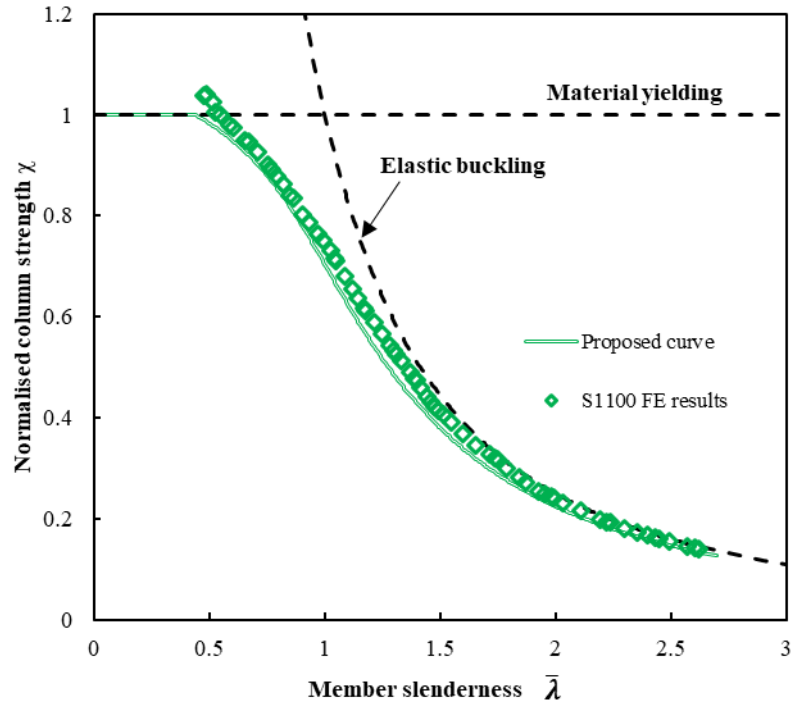




(a)

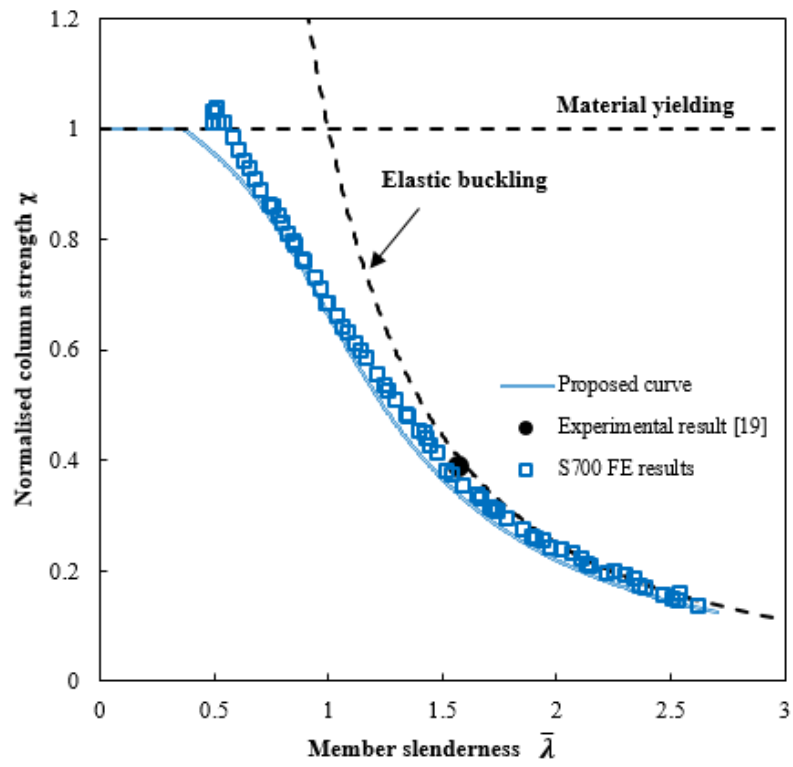


(b)

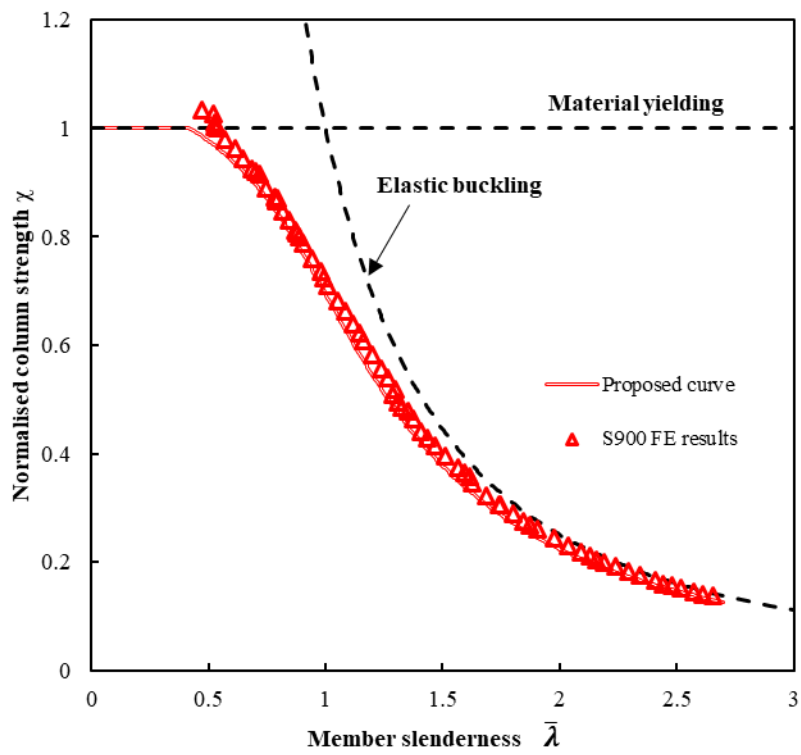


(c)

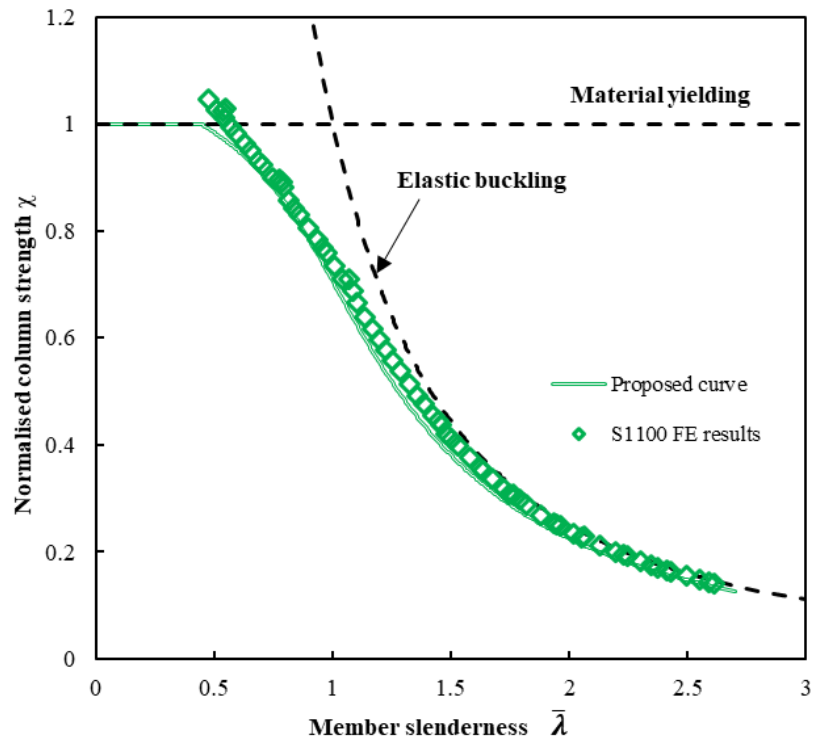
**Figure 16.** Comparison of the proposed column buckling curve with experimental and FE results for RHS columns buckling about major axes. (a) S700; (b) S900 and (c) S1100.



(a)

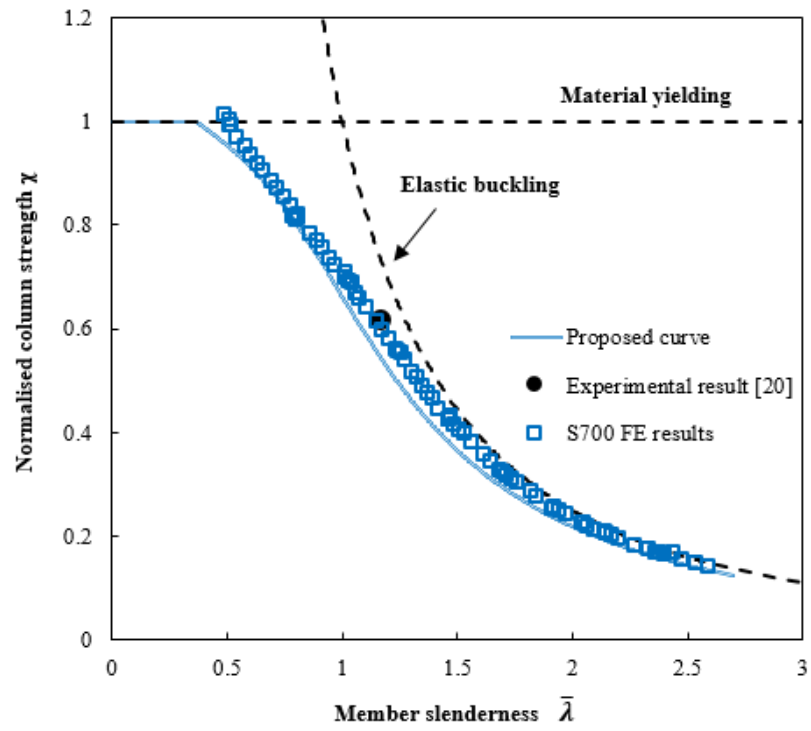


(b)

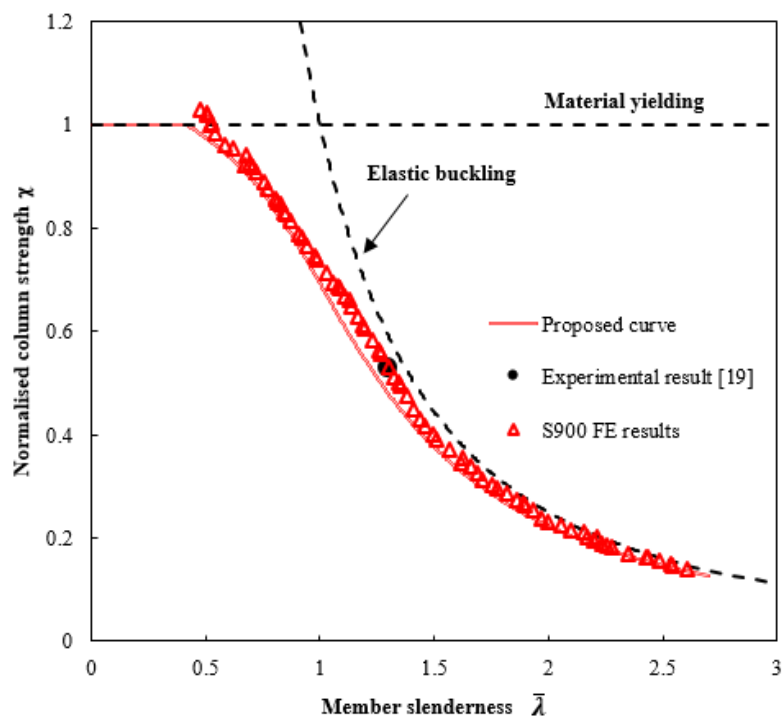


(c)

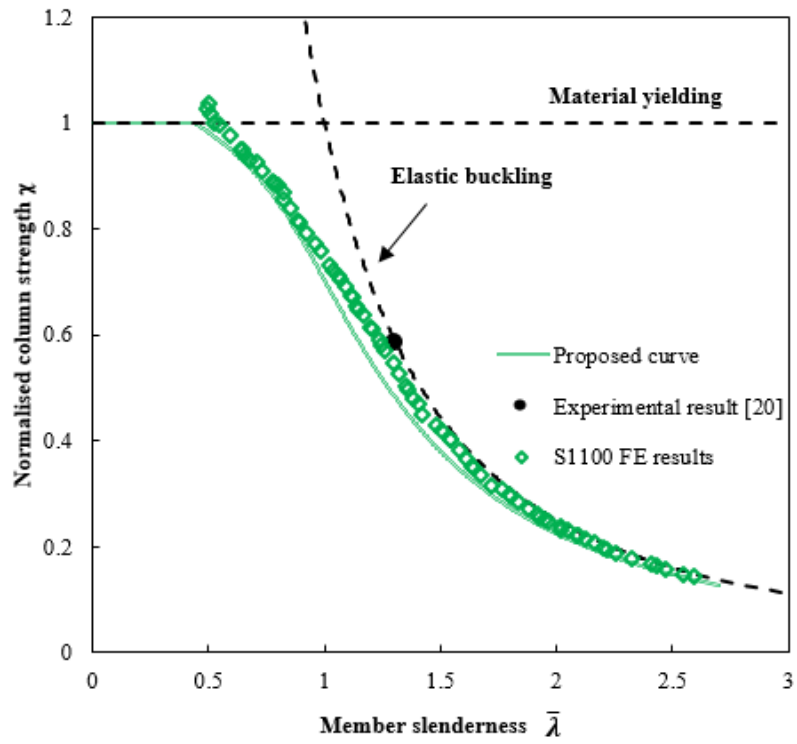
**Figure 17.** Comparison of the proposed column buckling curve with experimental and FE results for RHS columns buckling about minor axes. (a) S700; (b) S900 and (c) S1100.



(a)



(b)



(c)

**Figure 18.** Comparison of the proposed column buckling curve with experimental and FE results for CHS columns with steel grade of (a) S700; (b) S900 and (c) S1100.

**Table 1.** Labels, dimensions and test data of the SHS and RHS columns.

Specimen	B (mm)	H (mm)	t (mm)	R (mm)	L <sub>eff</sub> (mm)	N <sub>u,test</sub> (kN)	Flat portion		Corner	
							f <sub>y</sub> (MPa)	f <sub>u</sub> (MPa)	f <sub>y</sub> (MPa)	f <sub>u</sub> (MPa)
CF7- R150*8_1B [17]	151.3	151.3	7.88	20	2140	2852.0	751	834	815	951
CF9- R120*6_3B [17]	120.3	120.0	6.05	14	2940	1554.0	1088	1182	1109	1271
CF9- R150*7_2B [17]	151.3	151.2	6.85	16	2940	2876.0	1114	1199	1215	1399
CF9- R150*7_1A [17]	152.4	151.6	6.90	16	1840	4237.0	1114	1199	1215	1399
H 80*80*4- LBC [19]	80.3	80.1	3.94	9.5	1655	581.9	719	840	897	983
H 50*100*4- LBC [19]	50.3	100.2	3.98	8.5	1655	642.3	719	840	897	983
H 100*50*4- LBC [19]	100.2	50.6	3.97	8.5	1655	306.9	719	840	897	983

**Table 2.** Labels, dimensions and test data of the CHS columns.

Specimen	D (mm)	t (mm)	L <sub>eff</sub> (mm)	N <sub>u,test</sub> (kN)	f <sub>y</sub> (MPa)	f <sub>u</sub> (MPa)
165.1*3.0L1500 [18]	165.1	3.00	1500	733.0	485	545
165.1*3.0L2000 [18]	165.1	3.00	2000	661.0	485	545
220.0*3.5L2000 [18]	220.0	3.50	2000	1040.0	494	557
220.0*3.5L2500 [18]	220.0	3.50	2500	997.0	494	557
V89*3-LBC [19]	89.0	2.94	1655	444.4	1054	1116
S-HST2 [20]	76.1	3.20	1400	368.0	772	847
S-UHST2 [20]	76.1	3.20	1400	584.0	1247	1385



**Table 3.** Parameters values for SHS, RHS and CHS columns for parametric studies.

Cross-section shape	Parameter	Values	Fixed value
SHS	B (mm)	150	-
	H (mm)	150	-
	t (mm)	5.5 and 6.0 (for S700 members), 6.5, 7.0, 7.5, 8.0, 8.5, 9.0 and 10.0 (for S900 and S1100 members)	6.5
	Member slenderness	0.46~2.60	0.46, 0.70, 0.94, 1.18, 1.42, 1.66, 1.90, 2.14, 2.38, 2.60
	Steel grade	S700, S900, S1100	-
	Global geometric imperfection/column length	1/1000, 1/1580 (average ratio), 1/2000	1/1580
RHS	B (mm)	200	-
	H (mm)	100	-
	t (mm)	7.5 and 8.0 (for S700 members), 8.5 (for S700 and S900 members), 9.0, 9.5, 10.0, 10.5, 11.0 and 11.5 (for S900 members), 12.0 (for S1100 member)	10.0
	Member slenderness	0.46~2.60	0.46, 0.70, 0.94, 1.18, 1.42, 1.66, 1.90, 2.14, 2.38, 2.60
	Steel grade	S700, S900, S1100	-

	Global geometric imperfection/column length	1/1000, 1/1580 (average ratio), 1/2000	1/1580
	Buckling axis	Major and minor buckling axes	-
CHS	D (mm)	100	-
	t (mm)	4.0, 4.5 and 5.0 (for S700 members), 5.5, 6.0, 6.5 7.0, 7.5, 8.0, 9.0 and 10.0 (for S900 and S1100 members)	6.0
	Member slenderness	0.46~2.60	0.46, 0.70, 0.94, 1.18, 1.42, 1.66, 1.90, 2.14, 2.38, 2.60
	Steel grade	S700, S900, S1100	-
	Global geometric imperfection/column length	1/1000, 1/1280 (average ratio), 1/2000	1/1280

**Table 3/8**

**Table 4.** Material parameters for HSS steel in cold-formed cross-sections [25].

HSS material	E (GPa)	$f_y$ (MPa)	$f_u$ (MPa)	$\epsilon_u$ (%)	$f_u/f_y$ lower limit	$f_u/f_y$ upper limit
S700-flat	212	719	840	4.3	1.12	1.22
S700-corner	212	897	983	1.6	1.07	1.12
S700-CHS	214	772	816	4.6	1.05	1.12
S900-flat	208	982	1149	2.1	1.14	1.20
S900-corner	209	1138	1245	2.2	1.07	1.09
S900-CHS	210	1054	1116	2.3	1.09	1.12
S1100-flat	205	1073	1356	2.0	1.12	1.26
S1100-corner	206	1245	1470	2.1	1.07	1.18
S1100-CHS	207	1152	1317	2.2	1.09	1.36

**Table 5.** Comparisons of experimental and FE results with the design strength predictions for SHS columns and suggested selection of column buckling curves.

Steel grade	Parameters	EC3			AS4100		AISC 360	Proposed
		$\frac{\chi_{Exp+FE}}{\chi_{EC3,c}}$	$\frac{\chi_{Exp+FE}}{\chi_{EC3,b}}$	$\frac{\chi_{Exp+FE}}{\chi_{EC3,a}}$	$\frac{\chi_{Exp+FE}}{\chi_{AS,\alpha_b=-0.5}}$	$\frac{\chi_{Exp+FE}}{\chi_{AS,\alpha_b=-1}}$	$\frac{\chi_{Exp+FE}}{\chi_{AISC}}$	$\frac{\chi_{Exp+FE}}{\chi_{pro}}$
S700	Mean	1.25	1.16	1.07	1.08	1.01	1.07	1.08
	COV	0.04	0.03	0.02	0.02	0.03	0.03	0.02
	$\phi$	1.00	1.00	1.00	0.9	0.9	0.9	0.9
	$\beta$	3.06	2.75	2.40	2.80	2.48	2.97	2.91
	Selected	b			$\alpha_b = -0.5$		-	-
S900	Mean	1.27	1.17	1.09	1.08	1.01	1.09	1.07
	COV	0.04	0.03	0.02	0.02	0.03	0.03	0.02
	$\phi$	1.00	1.00	1.00	0.9	0.9	0.9	0.9
	$\beta$	3.13	2.79	2.48	2.80	2.48	3.06	2.87
	Selected	b			$\alpha_b = -0.5$		-	-
S1100	Mean	1.28	1.18	1.10	1.08	1.01	1.09	1.05
	COV	0.06	0.05	0.03	0.03	0.02	0.02	0.02
	$\phi$	1.00	1.00	1.00	0.9	0.9	0.9	0.9
	$\beta$	3.11	2.78	2.51	2.78	2.51	3.07	2.79
	Selected	b			$\alpha_b = -0.5$		-	-

**Table 6.** Comparisons of experimental and FE results with the design strength predictions for RHS columns buckling about major axis and suggested selection of column buckling curves.

Steel grade	Parameters	EC3			AS4100		AISC 360	Proposed
		$\frac{\chi_{Exp+FE}}{\chi_{EC3,c}}$	$\frac{\chi_{Exp+FE}}{\chi_{EC3,b}}$	$\frac{\chi_{Exp+FE}}{\chi_{EC3,a}}$	$\frac{\chi_{Exp+FE}}{\chi_{AS,\alpha_b=-0.5}}$	$\frac{\chi_{Exp+FE}}{\chi_{AS,\alpha_b=-1}}$	$\frac{\chi_{Exp+FE}}{\chi_{AISC}}$	$\frac{\chi_{Exp+FE}}{\chi_{pro}}$
S700	Mean	1.22	1.13	1.05	1.07	1.00	1.07	1.06
	COV	0.05	0.04	0.03	0.03	0.03	0.03	0.02
	$\phi$	1.00	1.00	1.00	0.9	0.9	0.9	0.9
	$\beta$	2.93	2.61	2.30	2.74	2.44	2.97	2.83
	Selected	b			$\alpha_b = -0.5$		-	-
S900	Mean	1.24	1.16	1.08	1.08	1.01	1.09	1.06
	COV	0.06	0.04	0.02	0.02	0.02	0.03	0.01
	$\phi$	1.00	1.00	1.00	0.9	0.9	0.9	0.9
	$\beta$	2.97	2.73	2.44	2.80	2.50	3.06	2.84
	Selected	b			$\alpha_b = -0.5$		-	-
S1100	Mean	1.26	1.17	1.09	1.08	1.02	1.11	1.06
	COV	0.06	0.05	0.03	0.03	0.02	0.02	0.02
	$\phi$	1.00	1.00	1.00	0.9	0.9	0.9	0.9
	$\beta$	3.04	2.74	2.47	2.78	2.54	3.15	2.83
	Selected	b			$\alpha_b = -0.5$		-	-

**Table 7.** Comparisons of experimental and FE results with the design strength predictions for RHS columns buckling about minor axis and suggested selection of column buckling curves.

Steel grade	Parameters	EC3			AS4100		AISC 360	Proposed
		$\frac{\chi_{Exp+FE}}{\chi_{EC3,c}}$	$\frac{\chi_{Exp+FE}}{\chi_{EC3,b}}$	$\frac{\chi_{Exp+FE}}{\chi_{EC3,a}}$	$\frac{\chi_{Exp+FE}}{\chi_{AS,\alpha_b=-0.5}}$	$\frac{\chi_{Exp+FE}}{\chi_{AS,\alpha_b=-1}}$	$\frac{\chi_{Exp+FE}}{\chi_{AISC}}$	$\frac{\chi_{Exp+FE}}{\chi_{pro}}$
S700	Mean	1.22	1.13	1.05	1.07	1.01	1.07	1.07
	COV	0.04	0.03	0.03	0.03	0.04	0.03	0.02
	$\phi$	1.00	1.00	1.00	0.9	0.9	0.9	0.9
	$\beta$	2.95	2.63	2.30	2.74	2.47	2.97	2.87
	Selected	b			$\alpha_b = -0.5$		-	-
S900	Mean	1.24	1.14	1.06	1.08	1.00	1.09	1.05
	COV	0.06	0.03	0.02	0.04	0.04	0.05	0.01
	$\phi$	1.00	1.00	1.00	0.9	0.9	0.9	0.9
	$\beta$	2.97	2.67	2.36	2.76	2.42	3.00	2.80
	Selected	b			$\alpha_b = -0.5$		-	-
S1100	Mean	1.25	1.17	1.09	1.08	1.02	1.11	1.06
	COV	0.06	0.05	0.03	0.03	0.02	0.03	0.02
	$\phi$	1.00	1.00	1.00	0.9	0.9	0.9	0.9
	$\beta$	3.00	2.74	2.47	2.78	2.54	3.14	2.83
	Selected	b			$\alpha_b = -0.5$		-	-

**Table 8.** Comparisons of experimental and FE results with the design strength predictions for CHS columns and suggested selection of column buckling curves.

Steel grade	Parameters	EC3			AS4100		AISC 360	Proposed
		$\frac{\chi_{Exp+FE}}{\chi_{EC3,c}}$	$\frac{\chi_{Exp+FE}}{\chi_{EC3,b}}$	$\frac{\chi_{Exp+FE}}{\chi_{EC3,a}}$	$\frac{\chi_{Exp+FE}}{\chi_{AS,\alpha_b=-0.5}}$	$\frac{\chi_{Exp+FE}}{\chi_{AS,\alpha_b=-1}}$	$\frac{\chi_{Exp+FE}}{\chi_{AISC}}$	$\frac{\chi_{Exp+FE}}{\chi_{pro}}$
S700	Mean	1.25	1.16	1.07	1.09	1.02	1.08	1.08
	COV	0.05	0.04	0.02	0.02	0.03	0.02	0.03
	$\phi$	1.00	1.00	1.00	0.9	0.9	0.9	0.9
	$\beta$	3.03	2.73	2.40	2.84	2.53	3.03	2.90
	Selected	b			$\alpha_b = -0.5$		-	-
S900	Mean	1.26	1.17	1.08	1.09	1.02	1.10	1.06
	COV	0.06	0.04	0.03	0.02	0.02	0.03	0.02
	$\phi$	1.00	1.00	1.00	0.9	0.9	0.9	0.9
	$\beta$	3.04	2.77	2.43	2.84	2.54	3.10	2.83
	Selected	b			$\alpha_b = -0.5$		-	-
S1100	Mean	1.27	1.18	1.09	1.09	1.02	1.11	1.06
	COV	0.06	0.05	0.03	0.02	0.02	0.03	0.02
	$\phi$	1.00	1.00	1.00	0.9	0.9	0.9	0.9
	$\beta$	3.07	2.78	2.47	2.84	2.54	3.14	2.83
	Selected	b			$\alpha_b = -0.5$		-	-